



Large wood loads in channels and on floodplains after a 500-year flood using UAV imagery in Mark Twain National Forest, Ozark Highlands, Missouri

R.T. Pavlowsky^{a,b}, J.W. Hess^{a,b,*}, D.J. Martin^c, T. Dogwiler^b, J. Bendix^d

^a Ozarks Environmental and Water Resources Institute, Missouri State University, Springfield, MO, United States of America

^b Department of Geography, Geology, and Planning, Missouri State University, Springfield, MO, United States of America

^c Department of Geography and Planning, Appalachian State University, Boone, NC, United States of America

^d Department of Geography and the Environment, Syracuse University, Syracuse, NY, United States of America

ARTICLE INFO

Keywords:

Floods
Riparian forests
Missouri Ozarks
Fluvial geomorphology
UAV imagery

ABSTRACT

Anthropogenic climate change has increased the frequency of large floods in rivers draining the Ozark Highlands. This study assesses the effects of a > 500-yr flood in spring 2017 on riparian forests and large wood loads in the North Fork of the White River watershed, Missouri, for six stream reaches with drainage areas from 5 to 124 km². Standing trees and large wood (LW) were assessed using unmanned aerial vehicle (UAV) imagery and calibrated by field surveys. Scaled flood magnitude (flood stage/bankfull depth) correlated with percent urban and agricultural land above each reach suggesting that land use may have contributed to forest damage. Canopy loss on the valley floor ranged from 7 to 63 % by reach and correlated with mean and cross-sectional stream power ($p < 0.01$). Standing tree density after the flood ranged from 50 to 243 trees/ha. The density of LW pieces ranged from 25 to 147 trees/ha. Most LW was aligned with stream flow, not in jams, and located on floodplains below riffles or bar heads, along channel bends, or in chutes. Wood loads on the valley floor increased downstream from 12 to 45 m³/ha. Channel loads were < 30 m³/ha while floodplain, terrace, and chute loads were > 30 m³/ha at drainage areas > 50 km². Channel LW loads increased with flood magnitude and in narrow valleys ($p < 0.02$), but not drainage area. Increased wood storage occurred on floodplains and terraces, but it is not clear if the stored wood will be available for downstream transport by future floods.

1. Introduction

Riparian forests grow along headwater streams and larger rivers on channel beds, floodplains, and terraces inundated by frequent or occasional flooding (Naiman and Decamps, 1997; Naiman et al., 2005). Their importance to sustaining biological diversity and structural integrity in fluvial systems is well recognized (Poff, 2002; Naiman et al., 2005; Steiger et al., 2005; Olson et al., 2007; Raeker et al., 2010). Moreover, riparian forests regulate the supply of large wood (LW) to channel systems and the cycling rates of LW between channels and floodplains (Latterell and Naiman, 2007; Wohl, 2013; Ruiz-Villanueva et al., 2016a, 2016b; Lininger et al., 2017; Wohl, 2017; Wohl et al., 2019). Through interactions with discharge and sediment, LW recruitment, deposition, and storage creates geomorphic heterogeneity, resilience, and habitat within channel systems (Keller and Swanson, 1979; Montgomery and

MacDonald, 2002; Montgomery et al., 2003; Naiman et al., 2005; Wohl, 2013; Solari et al., 2016; Wohl et al., 2019). Previous studies describing channel geomorphology have focused mainly on understanding the effects of hydrology and sediment pathways. Less attention has been put on understanding the role that LW plays in the regulation of geomorphic processes and the influence of human impacts on wood recruitment in the channel (Gurnell et al., 2002; Montgomery et al., 2003; Naiman et al., 2005; Wohl, 2017).

Large wood provides an array of important ecosystem services to support ecological functions, river restoration goals, and societal needs (Polednikova and Galia, 2021). Large wood is defined here as any downed wood including trunks, branches, root wads, or whole trees within the riparian zone including channels and adjacent floodplains that is at least 10 cm in width and 1.5 m in length (Wohl et al., 2019; Martin et al., 2021). Wood jams are local accumulations of three or more

* Corresponding author at: Ozarks Environmental and Water Resources Institute, Missouri State University, Springfield, MO, United States of America.
E-mail address: joshhess@missouristate.edu (J.W. Hess).

LW pieces in contact with each other (Keller and Swanson, 1979; Guiney and Lininger, 2021; Martin et al., 2021). Large wood can provide hydraulic roughness and erosional resistance in channels and on floodplains to increase flood water retention rates (Bren, 1993; Hauer and Smith, 1998), landform stability (Hupp and Osterkamp, 1996; Tal et al., 2004), and higher rates of deposition/filtration for sediments, nutrients, and pollutants (Vought et al., 1994; Daniels and Gilliam, 1996; Lowrance, 1998; Neary et al., 2010; Sutfin et al., 2016; Wohl and Scott, 2016; Vigiak et al., 2016). The geomorphic effects of LW can operate at multiple scales ranging from short-term adjustments of channel processes and sediment storage to longer-term controls on river profiles and basin erosion rates (Montgomery et al., 2003; Wohl, 2013).

Large wood deposition and storage in channels and on floodplains is typically measured in units of total volume (m^3) or volume per unit area or load (m^3/ha). Higher LW loads are typically deposited in stream segments with mature or productive forests, slow decay rates for downed wood, no history of forest clearing or harvesting, and frequent LW inputs from hillslopes, debris flows, or floods (Keller and Swanson, 1979; Johnson et al., 2000; Herring et al., 2004; Warren et al., 2009; Comiti et al., 2016; Lininger et al., 2017; Venarsky et al., 2018; Lapidés and Manga, 2020; Guiney and Lininger, 2021). Channel loads tend to decrease downstream with drainage area (or per unit drainage area) because of reduced slope or velocity, attenuation of the flood peak, and exhaustion of wood supplies (Kraft et al., 2002; Marcus et al., 2002; Wohl and Jaeger, 2009; Comiti et al., 2016; Ruiz-Villanueva et al., 2016a, 2016b). The highest rates of LW deposition and jam formation on channel beds tend to occur in headwater or small tributary streams where wood length exceeds bankfull width making free floating and unobstructed transport difficult (Keller and Swanson, 1979; Gurnell et al., 2002; Kramer and Wohl, 2017). In contrast, LW mobility tends to increase downstream as the channel widens and floods deepen thus depositing relatively more LW and jams along channel margins or on floodplains in comparison to mid-channel locations or on the channel bed (Marcus et al., 2002). Wood mobility tends to decrease in multi-threaded and branching channel types with greater number of channel and forest obstacles tend to trap or deposit larger LW loads compared to hydraulically smoother and deeper single-channel streams (Swanson et al., 1998; Scott and Wohl, 2018; Venarsky et al., 2018; Wohl et al., 2018). Floodplains in montane conifer watersheds along straight channels stored about one-third less the wood volume compared to multi-thread, braided, and meandering channels (Wohl et al., 2018).

Primary and secondary channels provide the primary conduits for LW transport. However, floodplain morphology, hydrology, and forest composition typically regulate LW budgets in streams (Wohl et al., 2019). Floodplains usually supply most of the wood to the channel, control wood cycling rates and residences times, and remove wood by decay, breakage, and burial (Wohl, 2013). The importance of floodplains as both a source and storage site for LW, nutrients, and carbon is poorly understood in many regions (Latterell and Naiman, 2007; Sutfin et al., 2016; Lininger et al., 2017; Wohl et al., 2018). Few studies have tried to describe how LW loads vary spatially across the valley floor with distance from the main channel (Gurnell et al., 2002; Wohl, 2013; Wohl et al., 2018; Ruiz-Villanueva et al., 2016a, 2016b; Lininger et al., 2017, 2021). This information is needed to develop bio-geomorphological models that include LW components to explain stream behavior in different regions (Wohl et al., 2010; Wohl, 2017; Wohl et al., 2019; Ruiz-Villanueva et al., 2016a, 2016b, 2019). Further, our knowledge of floodplain wood loads is limited regionally, since most studies of floodplain LW occurred in mountain watersheds in the western and northwestern USA (e.g., Swanson et al., 1998; Johnson et al., 2000; Friedman and Lee, 2002; Comiti et al., 2016; Wohl and Scott, 2016; Wohl, 2017; Wohl et al., 2018; Keys et al., 2018; Guiney and Lininger, 2021; Lininger et al., 2021).

Large wood loads on floodplains can vary regionally by over an order of magnitude according to climate-vegetation associations, and they vary locally because of forest history, land use, flood regime, and valley

and channel geomorphology (Lininger et al., 2017; Huylenbroeck et al., 2021). At the regional scale, average LW loads on floodplains generally increased by biome type as follows: tropical wet ($10 \text{ m}^3/\text{ha}$) (Chao et al., 2008), tropical dry ($15 \text{ m}^3/\text{ha}$) (Jaramillo et al., 2003), and semiarid boreal ($42.3 \text{ m}^3/\text{ha}$), subtropical ($50.4 \text{ m}^3/\text{ha}$), and semiarid temperate ($116.6 \text{ m}^3/\text{ha}$) (Lininger et al., 2017). The highest loads have been reported for the temperate coniferous forest biome such as the Redwood forests in California, which stored an average of $743 \text{ m}^3/\text{ha}$ of LW on floodplains (Busing and Fujimori, 2005). Reported LW loads in channels broadly range from 5 to $800 \text{ m}^3/\text{ha}$ (Martin et al., 2021), varying by forest type as follows: deciduous, $20\text{--}100 \text{ m}^3/\text{ha}$; mixed, $80\text{--}300 \text{ m}^3/\text{ha}$; and conifer, $100\text{--}600 \text{ m}^3/\text{ha}$ (Ruiz-Villanueva et al., 2016a, 2016b).

Flood regime, particularly the magnitude and frequency of relatively large floods, is a major driver of floodplain dynamics, riparian forest structure, and wood loading (Bendix, 1997; Bendix and Hupp, 2000; Ruiz-Villanueva et al., 2016a, 2016b, 2019; Wohl et al., 2019). Over-bank floods can account for 70 % of the LW transport in watersheds (Kramer and Wohl, 2017). In mountain watersheds, infrequent-large magnitude floods can increase the supply of LW available for storage on floodplains by 10 to 20 times the pre-flood conditions (Bendix, 1994; Herring et al., 2004; Engelhardt et al., 2011; Scott and Wohl, 2018). In addition, more frequently flooded areas on the valley floor may accumulate wood loads up to two times greater than those found in less frequently flooded areas (Lininger et al., 2017). Pre-event factors can influence the recruitment of LW by floods including forest type, amount and size of wood stored and available for transport, and geomorphic boundary conditions such as valley width, channel type, and relief (Johnson et al., 2000).

Riparian tree damage and LW recruitment by floods is expected to increase in relatively narrow, straight, and steep valley channels where flood currents are unimpeded and impact standing trees with more force, frequently remove downed trees, and result in relatively younger stands over time (Swanson et al., 1998). Floods generating high stream power can align free or root-anchored logs parallel to banks or fast currents with root wads upstream (Johnson et al., 2000; Kramer and Wohl, 2017). Conversely, more mature stands are found in valleys with broad floodplains and secondary channel systems that can spread out and pool flood waters to dissipate hydraulic energy and provide greater capacity for wood deposition (Swanson et al., 1998; Johnson et al., 2000; Guiney and Lininger, 2021; Wohl and Iskin, 2022). Stream power, and thus forest damage, can fluctuate downstream during a large flood because of variations in flood routing, local stage height, and channel widening (Ruiz-Villanueva et al., 2018). Understanding the effects of large floods on LW dynamics is timely since flood magnitude and frequency have been increasing over the past 30 to 50 yr in many regions worldwide (Poff et al., 1996; Chang et al., 2002; Andréasson et al., 2004; Slater and Villarini, 2016; Alfieri et al., 2017; Wing et al., 2022).

Human activities have significantly decreased riparian forest area and stream wood loads in many watersheds around the world (Naiman et al., 2005; Steiger et al., 2005; Kondolf et al., 2007; Seavy et al., 2009; Perry et al., 2012). In the USA, <5 % of all old growth forests remain with 70 % of riparian forests having been converted to agriculture and other uses (Meyer, 1995; Turner et al., 1998). Wood loads have decreased in the USA over the past 100 to 200 yr in rivers flowing through populated areas or other areas managed for agriculture, irrigation, flood control, transportation/navigation, or recreation uses (Christensen et al., 1996; Latterell and Naiman, 2007; Wohl et al., 2019; Guyette et al., 2008; Blaich and Jefferson, 2019). On-going reductions in wood loads to streams can increase the frequency of bedrock channels (Montgomery et al., 1996), decrease the number of pools and riffles (Montgomery et al., 1995), and transform multithreaded channels to single channel forms (Montgomery and Abbe, 2006; Collins et al., 2012; Wohl, 2013). It can take more than two centuries for wood loads to recover by natural regeneration after the removal or “de-snagging” of LW from a channel system (Christensen et al., 1996; Stout et al., 2018).

The present study addresses gaps in our understanding about how

extreme floods can damage riparian forests, recruit new wood, and deposit LW in channel and floodplain areas (Swanson et al., 1998; Johnson et al., 2000; Hu et al., 2005; Kramer et al., 2008; Garssen et al., 2015, 2017; Comiti et al., 2016; Wohl, 2017; Dwire et al., 2018; Martinez-Fernandez et al., 2018; Lininger et al., 2021; Wu et al., 2021). Further, it fills a regional gap in floodplain LW studies by quantifying the spatial distribution and geomorphic relationships of channel and floodplain wood loads in tributary streams (4–124 km²) to the North Fork of the White River in south-central Missouri, USA, after the occurrence of the largest flood on record in April 2017 (Heimann et al., 2018; Martin et al., 2021). Three objectives addressed are to: (i) use hydro-geomorphic methods to classify valley floor landforms and reconstruct flood stage and discharge at six study reaches in the North Fork watershed; (ii) describe variations in forest damage and LW characteristics among valley floor landforms; and (iii) quantify channel and floodplain LW loads to evaluate the influence of flood and geomorphic factors on downstream and cross-valley LW deposition and storage rates. Unmanned aerial vehicle (UAV) imagery is used to assess LW size and distribution. This application can provide a cost-effective option for collecting high-resolution aerial imagery in inaccessible or hard to reach areas (Quilter and Anderson, 2000; Anderson and Gaston, 2013). A companion study of the same sites in the North Fork watershed was

completed to assess post-flood in-channel wood transport and deposition through analysis of a different dataset derived from field measurements and not the remote UAV methods used here (Martin et al., 2021).

The North Fork watershed (1453 km²) drains the Salem Plateau of the Ozark Highlands (Ozarks) with a temperate subtropical climate, local relief up to 165 m, and mixed oak-pine forests interspaced with pasturelands on uplands and wider valley floors not in public ownership in Mark Twain National Forest (Fig. 1) (Adamski et al., 1995; Nigh and Schroeder, 2002). Flood magnitude, valley geomorphology, and channel type are probably the most important controls on wood transport and storage in these forested watersheds with narrow valley floors and flashy flood hydrographs (Ruiz-Villanueva et al., 2016a, 2016b; Martin et al., 2021). Wood debris inputs from hillslopes are rare in the Ozarks (Thornberry-Ehrlich, 2016). Other studies concluded that bank erosion can be the main source of wood to a stream (Morche et al., 2007). Therefore, it is hypothesized that LW recruitment is expected to come largely from along main channels where fast-moving currents: (i) remobilize stored wood from the channel and banks, (ii) increase the rates of channel widening and tree uprooting by bank erosion, and (iii) increase the frequency of tree collisions by floating wood or falling trees (Swanson et al., 1998; Johnson et al., 2000; Lininger et al., 2017; Meitzen et al., 2018). Further, it is also expected that riparian damage

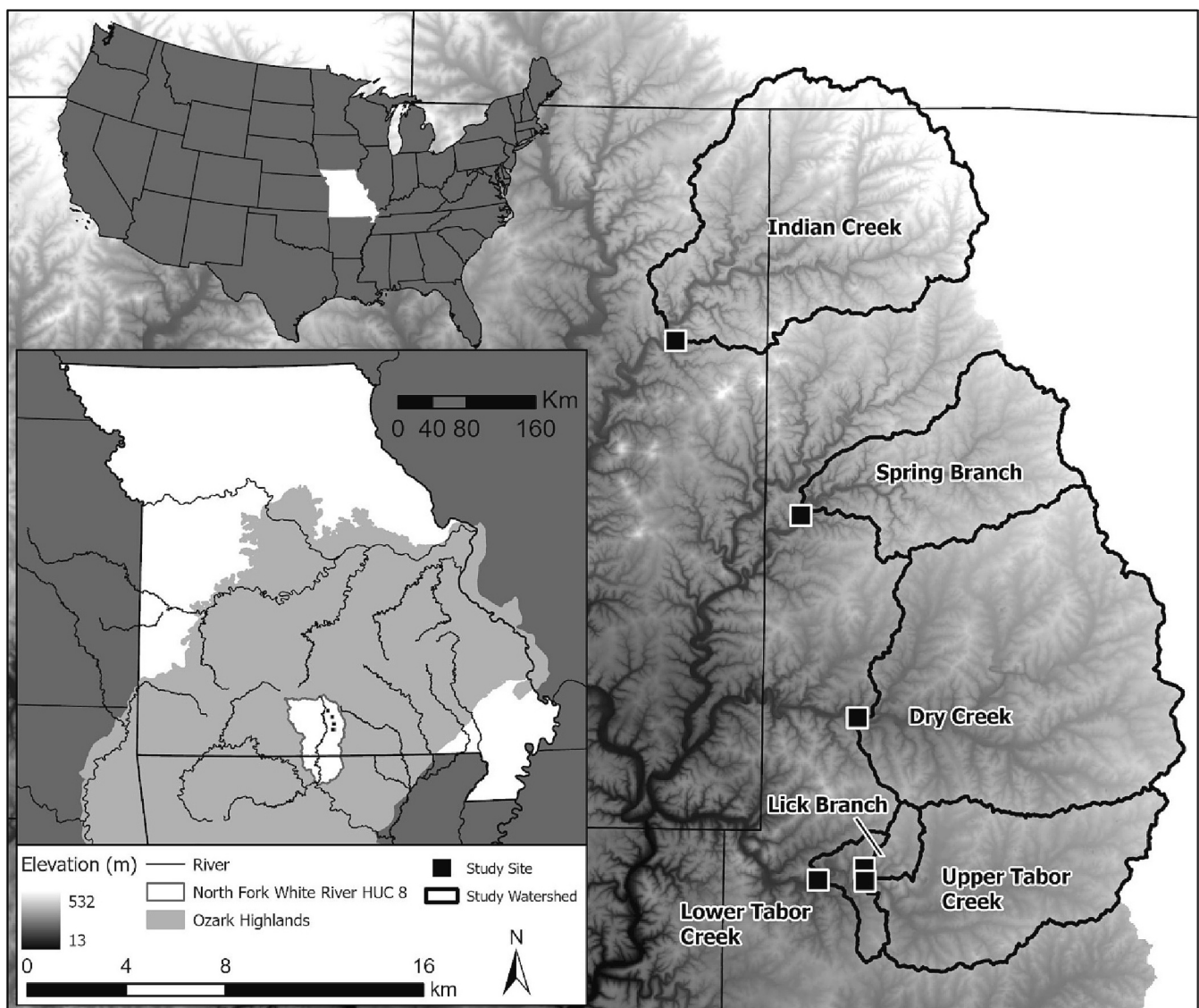


Fig. 1. Study area and sampling sites.

and supply of LW to floodplains will increase with local flood peak stage and depth of floodplain (Ruiz-Villanueva et al., 2018). Flood magnitude interaction with valley floor topography may represent the most important controls on LW load patterns for a given river morphology since forest damage, wood transport rates, and depositional zones are all influenced by the peak flood stage (Ruiz-Villanueva et al., 2016a, 2016b; Wohl et al., 2018).

In the Ozark Highlands, multithread channel systems occur in some headwater drainages that have been protected from or overlooked by human disturbance. However, single channel forms are more common, often with secondary channel systems, composed of bar and floodplain chutes of variable sizes branching laterally from the main channel across the valley floor (Panfil and Jacobson, 2001; Martin and Pavlowsky, 2011). Chutes form in sinuous or meandering reaches where higher velocity overbank flows can maintain an incised channel such as in backswamps and along the flanks of bars (Harrison et al., 2015). Valley floors with chute channels can have almost twice the wood storage volume of single channel reaches, with wood deposition occurring at entrances, bends, and shallow areas of chutes (Nakamura and Swanson, 1994). Therefore, it is hypothesized that LW loads and jams will be concentrated in relatively wide reaches where secondary channel development and associated flow separation zones occur (Scott and Wohl, 2018; Swanson et al., 1998; Venarsky et al., 2018; Wohl et al., 2018). In the study area, chute channels typically occur along the inside of valley or channel bends with inlets occurring near channel constrictions at bar or riffle heads. In addition, it is expected that the distribution of LW loads will transition with increasing drainage area from mainly channel deposition in smaller streams to more diverse channel and floodplain storage downstream in response to wider valleys and deeper overbank flood depths (Marcus et al., 2002; Wohl and Jaeger, 2009).

2. Study area

The North Fork of the White River (North Fork) (1453 km²) drains south-central Missouri (Fig. 1). It flows south about 100 km from a maximum elevation of 470 m near Mountain Grove, Missouri, to Tecumseh, Missouri, on Norfork Lake with an average pool elevation of 170 m. The present-day land use of the North Fork watershed is mostly forest (63 %) and pastureland (28 %), with <4 % covered by urban areas (Multi-Resolution Land Characteristics (MRLC) Consortium, 2016). This study assessed six sample reaches (5–124 km²), including stream channel and valley floor areas, located along North Fork tributaries within the Willow Springs District of Mark Twain National Forest (Miller and Wilkerson, 2001) (Table 1, Figs. 1 & 2).

Sample reaches are underlain by horizontally bedded sandstones and dolomites of Ordovician and Mississippian age in the Salem Plateau of the Ozarks Highlands (Adamski et al., 1995; Miller and Wilkerson, 2001). Karst features such as sinkholes, caves, springs, and losing streams are found throughout the region and near the study sites (Miller and Wilkerson, 2001; Duley et al., 2015). Upland soils are typically alfisols and ultisols formed in a thin (<1 m) mantle of Pleistocene loess overlying cherty and clayey residuum on limestone and dolomite bedrock (Miller and Wilkerson, 2001). Alluvial soils include entisols formed on active bar and bench features composed of sand and gravel (Relfe and Sandbur series), alfisols formed on floodplains with a fine-textured overbank unit 0.5–1 m thick overlying a gravelly channel unit (Secesh and Tilk series), and alfisols on terraces composed of similar parent materials as floodplains but with more developed soil horizons (Britwater series) (USDA, 2005; USDA, 2006). Bedrock is often exposed along the lower banks and channel beds of tributary streams (USDA, 2006).

Annual precipitation in the watershed averaged 110 cm, ranging from 52 cm to 166 cm, for the period of 1946 to 1995 (Adamski et al., 1995; Miller and Wilkerson, 2001). The annual precipitation in 2018 was 132 cm in West Plains, Missouri, located in the eastern part of the watershed (MRCC, 2019). The spring months of March, April, and May

Table 1
Sample reach characteristics.

Variable	Dry Creek	Indian Creek	Lower Tabor Creek	Upper Tabor Creek	Spring Branch	Lick Branch
Watershed Characteristics						
Drainage Area (km ²)	124.2	101.6	65.4	54	49.1	4.5
Elevation (masl)	268	250	262	288	273	291
Basin Slope (m/m)	0.006	0.007	0.013	0.005	0.008	0.013
Area in MTNF (%)	36	43	19	7	50	62
Agriculture (%)	31	16	45	52	19	13
Forest (%)	64	79	50	42	78	86
Urban (%)	4	3	4	5	2	1
Other (%)	1	2	1	1	1	0
Reach Characteristics						
Reach Length (m)	303	470	766	404	424	119
Reach area (ha)	2.1	4.0	4.8	2.0	3.4	0.3
Length:BF width ratio	15	15	16	14	16	9
Channel type	single losing	single peren.	single losing	multi losing	single peren.	multi ephem.
Hydrology Sinuosity (m/m)	1.09	1.14	1.70	1.02	1.28	1.08
Valley Width (m)	103	101	57	66	128	59
Confinement Ratio	5.2	3.2	2.5	2.3	4.9	4.4
Post-flood Bankfull Channel Morphology						
Width (m)	19.9	31.5	23	28.6	25.8	13.3
Depth Max (m)	2.13	2.19	1.39	1.40	1.56	0.71
Depth Mean (m)	1.56	1.44	0.92	0.88	0.75	0.45
Width:Depth Ratio	12.8	21.9	25.0	32.5	34.4	29.6
Reach Slope (m/m)	0.007	0.003	0.010	0.005	0.004	0.015
Manning's n	0.045	0.040	0.045	0.040	0.045	0.075
Bankfull Discharge						
(m ³ /s)	69.5	62.2	42.5	36.6	38.3	7.6
Bed diameter (D50, mm)						
	35	40	49	16	28	64
Max Clast (avg., mm)						
	512	166	286	196	108	182

typically receive the most precipitation at >12 cm per month, while winter months of December, January, and February and the mid-summer month of July receive the least at <8 cm per month (climate-data.org). The frequency of more intense rains (>7.5 cm/day) has increased significantly in the Ozark Highlands over the past 30 yr because of the influence of recent climate changes linked to global warming thus increasing runoff and annual peak flood discharges (Hu et al., 2005; Pavlowsky et al., 2016; Slater and Villarini, 2016; Flanagan and Mahmood, 2021). On average, the annual peak discharge of the larger rivers in the vicinity of the study area has been increasing at 2 to 4 % per year from 1975 to 2017 (Heimann et al., 2018). The USGS discharge gaging station on the North Fork near Tecumseh, Missouri (1453 km²), has been in operation since 1945 with a mean annual discharge for the period of record of 21.3 m³/yr. Of the ten highest annual flood peaks on record, five have occurred since 2000, with four

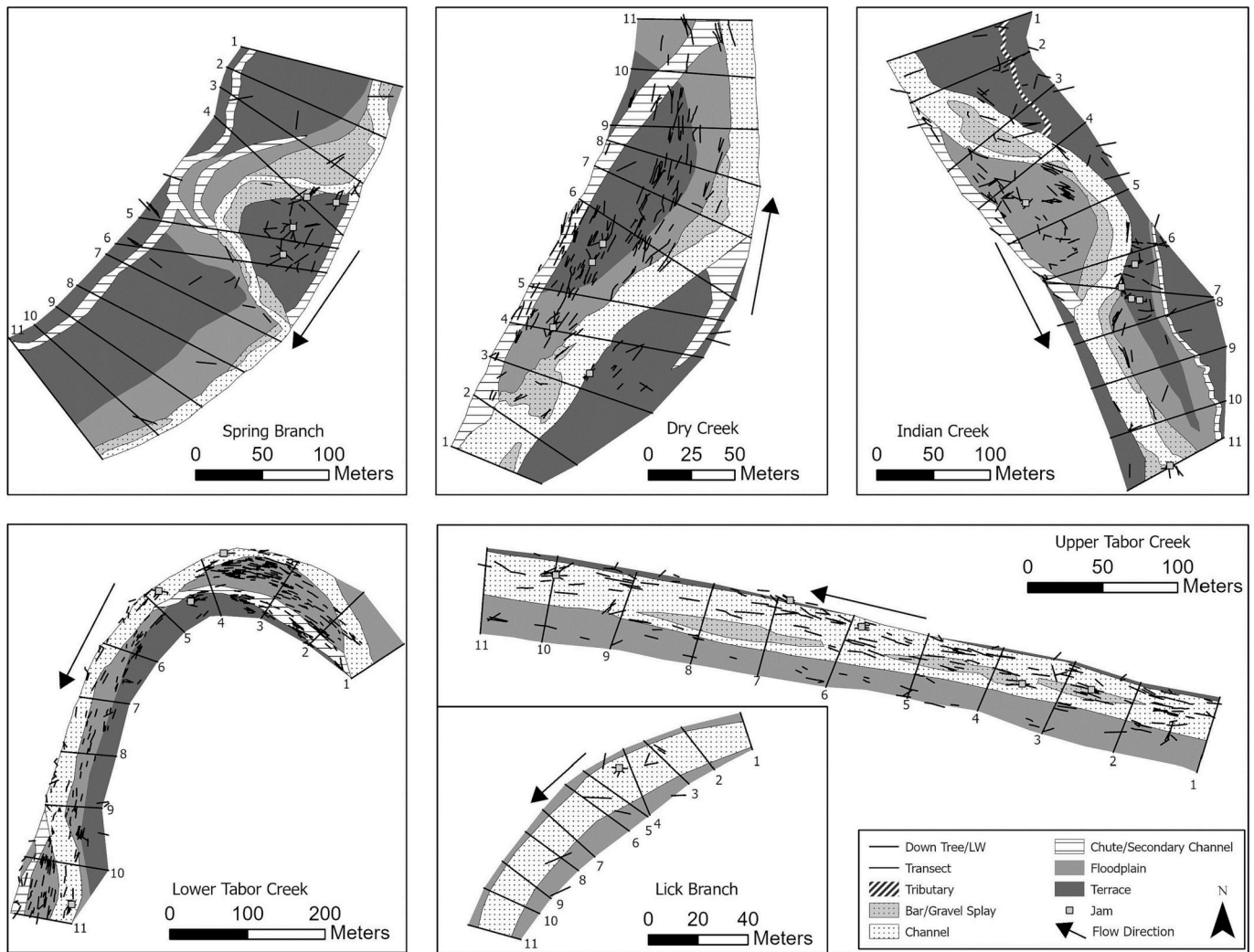


Fig. 2. Landforms and large wood in sample reaches.

during 1980–1999, and one during 1970–79. On April 28–30, 2017, the North Fork watershed received 20 to 30 cm of rainfall, which produced the largest flood peak of record at 5352 m³/s with a stage of 12.7 m described as the >500-yr event (Erdman, 2017; US Department of Commerce, 2017; Heimann et al., 2018).

The North Fork watershed is in the temperate broadleaf and mixed forest biome. Pre-settlement forest composition was mostly pine, pine-oak, and oak-pine forest (Sauer, 1920; Raeker et al., 2010). In the 1850s, shortleaf pine logging began along tributaries of the North Fork River in Ozark, Douglas, and Howell Counties (Sauer, 1920). These “pineries” yielded logs 24 to 27 m in length and up to 1.2 m in diameter (Sauer, 1920; Guldin, 2008). Between 1880 and 1920, exploitive pine logging and timber production spread throughout the eastern and central Ozark Highlands in Missouri. Oak and other hardwoods were harvested after the pine was depleted (Jacobson and Gran, 1999; Guldin, 2008). Historical soil and vegetation disturbances during early Euro-American settlement followed by expansion of cultivated land and logging after the Civil War increased runoff, suspended sediment supply, headwater stream incision, and gravel loads in Ozark streams during the period from 1880 to 1930 (Sauer, 1920; Jacobson and Gran, 1999; Miller and Wilkerson, 2001; Martin and Pavlowsky, 2011; Owen et al., 2011). Since the early 1800s, forest clearance related to settlement expansion, agriculture, and logging led to fuel fragmentation and lower forest fire frequency until 1920 when fire was actively suppressed (Nanavati and Grimm, 2020). Post-settlement legacy deposits have been

identified on floodplains along the main valley of the North Fork (Ray, 2009).

Forest management began in the 1930s when the US Forest Service acquired extensive tracts of cut-over and unproductive lands to form what is now called the Mark Twain National Forest (Guldin, 2008). Since 1939, cutting frequency (i.e., tree age at harvest) in government managed forests has generally been 80 to 100 yr, but as young as 10 to 50 yr. Logging typically occurred on 10 to 30 ha stands with at least 10 % of the “old growth” or mature trees left standing (Brookshire et al., 1997). Historical aerial photography indicates that no logging has occurred within the study reaches and adjacent drainage areas for at least the past 40 to 50 yr. Prescribed burning in or around sample reaches was not reported on Forest Service schedules. Further, no evidence of burned wood was found at any of the six sample reaches. Presently, the dominant canopy species of upland forests include various oak (*Quercus*) and hickory (*Carya*) species and shortleaf pine (*Pinus echinata*) (Stambaugh et al., 2002). The five most common canopy species inventoried on valley floor transects for this study were White Oak (*Quercus alba*) (43 %), Shortleaf Pine (*Pinus echinata*) (10 %), American Sycamore (*Platanus occidentalis*) (9 %), other oaks (*Quercus* sp.) (9 %), and White Ash (*Fraxinus americana*) (7 %). These species (except shortleaf pine) were identified by managers as important riparian trees in the Ozark Highlands (Steele et al., 2013).

3. Methods

3.1. Field methods

Six sample reaches were selected for study based on: (i) targeting tributaries draining a high rainfall area in the northeast portion of the North Fork watershed, (ii) sampling a range of drainage areas, and (iii) accessibility to national forest lands (Table 1; Figs. 1 & 2). The reaches were assessed for channel morphology, flood stages and stream power, valley floor morphology, stranding tree density and large wood density (trees/ha) and volume or load (m^3/ha).

Initial geomorphologic assessments occurred September 2017 about 4.5 months after the flood (Martin et al., 2021). Discharge records at the Tecumseh gage indicated that no significant runoff events occurred in the North Fork watershed since the April 2017 flood. Sample reaches were approximately 20 active channel widths in length with channel data collected from 11 transects spaced at intervals of two channel widths (Fig. 2) (Harrelson et al., 1994; Rosgen, 1996; Panfil and Jacobson, 2001). Channel data were collected on the type, height, and width of bed and bar features, bank height along the channel, and other valley floor landforms including benches, bars, and secondary channels/chutes using a tape/stadia rod, hand-level, and Trimble Geo7t GPS receiver. Pebble counts of 30 blind-touch samples were completed by gravelometer using a paced grid to determine the median diameter (D50) for 1–2 riffles in each reach (Wolman, 1954; Bunte and Abt, 2001). The diameters of the five largest mobile clasts deposited in the riffle crest were also recorded. The heights of high-water marks (HWM) from tree scars and strand lines were measured and used to estimate flood stages above the bed elevation (Morche et al., 2007). Large wood tallies were completed for the channel with the methods and results previously reported in Martin et al. (2021).

In August 2018, the six sample reaches were revisited to survey valley cross sections using an auto-level and pulled tapeline to measure channel dimensions, floodplain and terrace elevations, and landform locations (Rosgen, 1996). Longitudinal profiles were also completed to calculate reach slopes and identify channel bedforms and their relationships to floodplain features (Rosgen, 1996). Geospatial coordinates and elevations for leveling surveys were determined using GPS and UAV digital surface models (DSMs) (described below). Two bankfull or 1.5-yr recurrence interval (RI) floods occurred during the 11-month period between the initial channel assessments in September 2017 and the auto-level cross section and longitudinal surveys in August 2018.

The use of UAV imagery for LW assessments had three field components: (i) collection of UAV imagery on September 2017 (leaf-on) to assess canopy loss at each sample reach; (ii) collection of UAV imagery on March 2018 (leaf-off) to assess valley floor topography, landform distribution, and standing trees and downed large wood locations and size, and (iii) field sampling of tree and LW locations and size from one to three transects at each sample reach in April 2019 to verify UAV accuracy (UAV analysis procedures described below). One bankfull event (1.5-yr RI) occurred during the 10-month period between the April 2017 flood and the March 2018 UAV flights.

In April 2019, ten field surveys of LW deposited in channel and floodplain areas were used to verify measurements derived from UAV imagery (Fujita et al., 2003; Allen et al., 2012). Using a strip sampling method (Lininger et al., 2017), standing trees and downed wood were assessed along a pulled tapeline transect extending across the entire valley floor within a sampling area of five meters in width. The locations and diameter at breast height were measured for standing trees (Kupfer et al., 2008; Stout et al., 2018). All downed wood positioned at a $< 45^\circ$ angle to the ground was assessed if the diameter was > 10 cm and length > 1.5 m (Brewer and Linnartz, 1973; Katz et al., 2005; Fierke and Kauffman, 2006; Chao et al., 2008; Kupfer et al., 2008; Lininger et al., 2017; Martin et al., 2018; Stout et al., 2018). Length was measured from the largest end of the wood piece, or top of the root wad, along the stem until the end of the piece or when the diameter decreased to 10 cm

(Stout et al., 2018). Diameter was measured at the midpoint of the recorded length (Cordova et al., 2007). Two sets of measurements were collected during transect surveys; one included only the length of wood extending at least 0.2 m into the 10-m wide grid for unit area volume calculations, and the second included the total length of the log and with adjusted mid-point/diameter locations to compare total piece length and diameter measurements between UAV and field methods. Only one bankfull event (1.5-yr RI) occurred during the 13-month period between UAV data collection and the ground-truthing field survey.

Large wood volume (m^3) was calculated assuming a cylinder shape for individual logs. Results for individual trees or LW pieces were tallied (counted) and evaluated in units of density (trees/ha), total volume as the product of length and diameter (m^3), and load per unit area (m^3/ha) (Ruiz-Villanueva et al., 2016a, 2016b; Wohl et al., 2019). The presence of wood jams in each grid was recorded where three or more pieces were in contact.

3.2. Geospatial data collection and analysis

Several imagery datasets were used in this study to describe watershed and reach characteristics. Watershed boundaries were delineated using the Hydrology toolset in ArcMap with a 10-m digital elevation model (DEM) released in April 2005 by the Missouri Spatial Data Information Service (MSDIS) (MSDIS, 2011). Watershed land use was assessed using the National Land Cover Database (NLCD) 2016 dataset, which provided 30 m resolution land cover data (MRLC, 2016). One-meter leaf-on aerial imagery for Douglas and Howell Counties, Missouri, collected during the peak agricultural growing season in 2016 by the National Agriculture Imagery Program (NAIP) was used to determine the area of pre-flood canopy coverage (USDA, 2016).

High-resolution (< 8 cm) UAV imagery was collected at all six sites with a DJI Phantom 4 Pro in September 2017 (leaf-on) and March 2018 (leaf-off). Loss of canopy cover by forest damage during the flood was assessed by the difference in digitized canopy areas between 2016 leaf-on NAIP imagery and post-flood September 2017 leaf-on UAV imagery (Everham and Brokaw, 1996; Stephens et al., 2008). During March 2018, about ten months after the flood, leaf-off UAV imagery was collected to assess LW size and distribution in channel, floodplain, terrace, and chute areas. According to regional stream gage records from main channel locations, probably only one near-bankfull event, and no overbank floods, occurred at the tributary sites used for this study during the period since the April 2017 flood.

To optimize spatial resolution, UAV imagery was processed using data collected from several flight plans at an altitude of 108 m with front and side image overlap of 80 % (Dandois et al., 2015; Jeong et al., 2018; Hostens et al., 2022). In addition, five to ten ground control points were used at each sample reach to geo-rectify UAV data (Vanlooy and Martin, 2005; Jeong et al., 2018). Structure-from-motion (SfM) photogrammetry software, Agisoft Metashape, was used to process UAV data and produce high resolution DSMs and orthoimages for each site (Hostens et al., 2022). SfM photogrammetry identifies tie points in photographs taken from many perspectives to create three-dimensional shapes of objects allowing for accurate measurements to be acquired from the final DSM or ortho-image (Fonstad et al., 2013; Warrick et al., 2017). Standing trees and LW were identified visually on UAV imagery and heads-up digitized in ArcMap with the following attributes: azimuth, presence of 3+ piece wood jam, length, diameter, and volume (Nakamura and Swanson, 1994). Azimuth was used to evaluate LW orientation and alignment with adjacent streamflow. Measurement procedures for length and diameter on UAV images were the same as those used for the grid field assessments but measured in the digital environment. Examples of the field conditions and large wood resolution prevalent during the study are shown by paired UAV images and field pictures of large wood (Fig. 3). Large wood accumulations in this study look similar to some of those reported for other regions (Wohl and Scamardo, 2022).

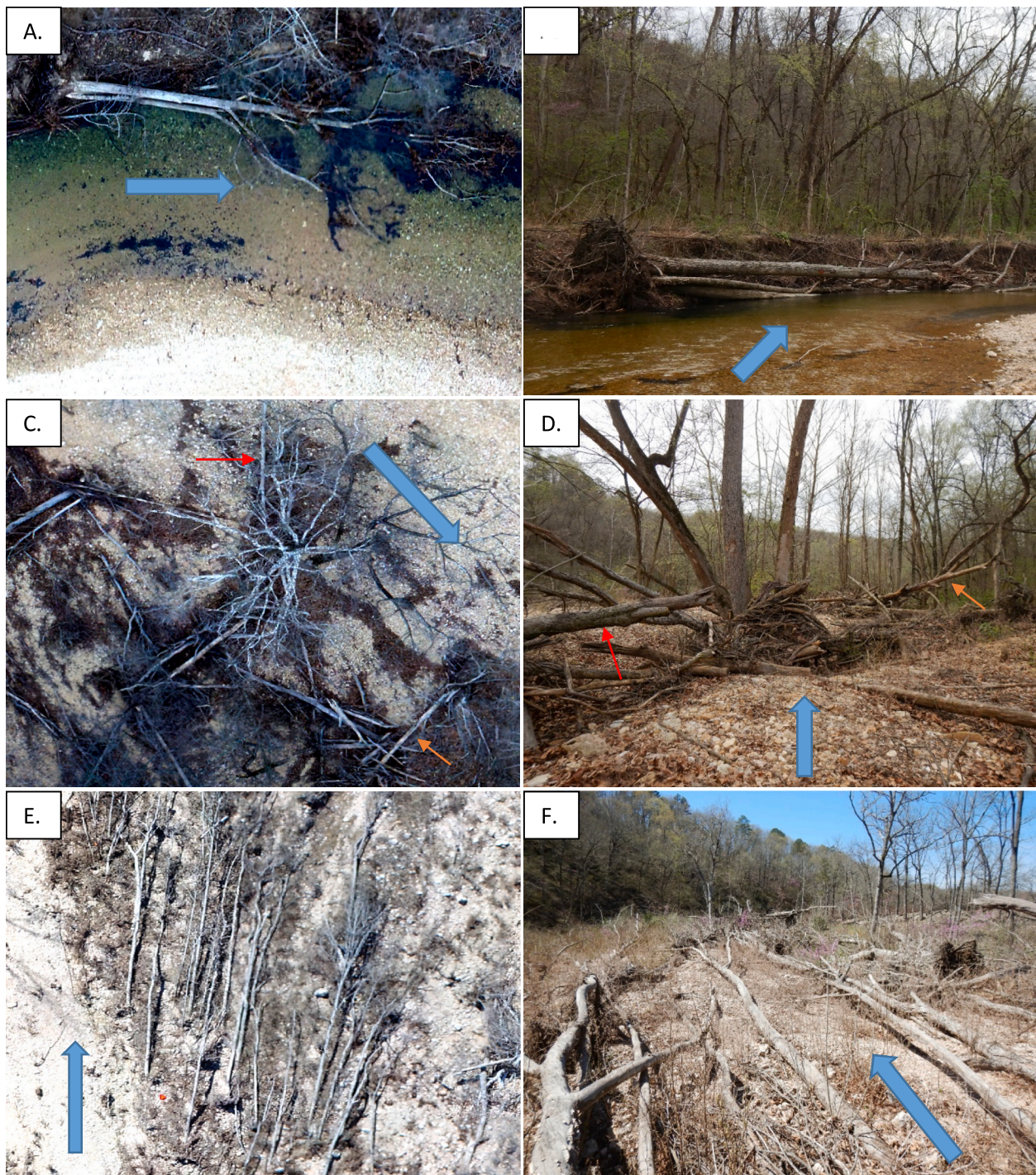


Fig. 3. Drone UAV and ground level pictures of large wood and reach conditions. Blue arrow indications flow direction during the flood. (A-B) 17 m long and 0.44 m diameter uprooted tree on the outside of a channel bend at Indian Creek. A, UAV imagery - 03/10/2018 & B, photograph - 03/10/2018). (C–D) Floodplain jam at Indian Creek. LW indicated in images is 9 m in length and 0.28 m diameter. C, UAV imagery - 03/10/2018 & D, photograph - 04/11/2019. (E-F) Uprooted/toppled trees aligned with streamflow on Lower Tabor Creek. Average tree length in the photo is 13 m. Most trees were toppled, remaining anchored by roots, and not transported. E, UAV imagery - 03/11/2018 & F, photograph - 04/12/2019. (G-H) Floodplain jam at Spring Branch. LW making “X” are 13 (bottom) and 14 (top) m in length and 0.37 and 0.42 m in diameter, respectively. G, UAV imagery - 03/10/2018 & H, photograph - 04/11/2019. (I) Large wood jam on standing tree key piece at Lower Tabor Creek. Bank is 4 m and jam is >2 m in height. Photograph - 09/21/2017. (J) Strand line debris and tree scar high water marks approximately 5 m above the channel bed at Upper Tabor Creek. LW in foreground is 10 m long and 0.32 m in diameter. Photograph - 09/21/2017.

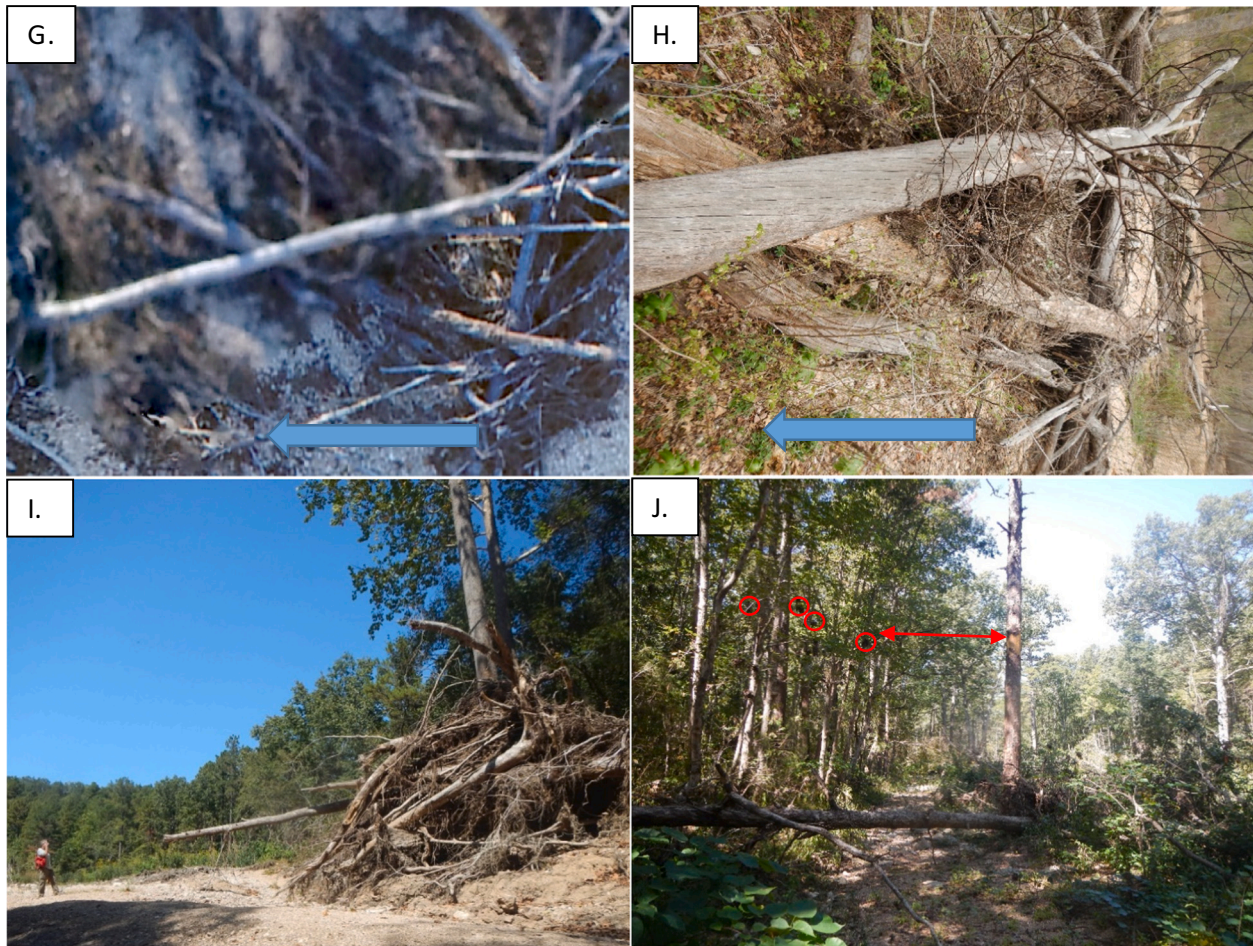


Fig. 3. (continued).

3.3. Correction of UAV results

Ground-truthing data analysis indicated that detection errors were present for some UAV measurements and that corrections could be made to calibrate UAV results with actual field data. Three variables were evaluated: (1) standing tree density (STD); (2) LW count or density; and (3) LW volume or load:

- (1) Paired field and UAV standing tree density (STD) values plot on a 1:1 line with an overall UAV detection accuracy was 98 %: $\text{Field} = 0.99 \times \text{UAV}$ ($n = 8$, $r^2 = 0.98$). No correction was used for the STD UAV data.
- (2) UAV imagery analysis underestimated LW counts (number per landform) and density (number per ha) by 30–50 % for field transects. Therefore, all LW density (trees/ha) values derived from UAV imagery were multiplied by a constant of 1.54, which is the median correction factor assuming an overall under-prediction error of 46 %. The interquartile range for the under-estimation factors from all sites was 16 % of correction factor.
- (3) UAV-based assessments underestimated LW volumes and loads overall by 30–70 %. Volume errors for LW using UAV imagery were mainly caused by lack of detection caused by visual obstruction and shadows and apparent shorter measured piece lengths caused by oblique resting positions and unclear log ends. Conversely, length measurements for flat-lying pieces and all diameter measurements from UAV images compared favorably with field data. Large wood volume or load values derived from UAV images were corrected using an equation that predicts the

ratio of the field value to UAV value (correction factor) based on the STD as follows: $\text{correction factor} = (0.0055 \times \text{UAV_STD}) + 0.93$; $r^2 = 0.40$ – 0.97 . It is reasonable to assume that detection error will increase with standing tree density since more overhead canopy cover will progressively obscure LW wood pieces underneath and offer more opportunity for oblique wood deposition.

Overall, 121 LW pieces were assessed by field methods with only 73 LW pieces identified using UAV imagery. Achieving 60 % detection for LW counts is reasonable recognizing that the present study used UAV imagery collected along transects through moderate to high levels of forest canopy. Using both UAV imagery and structure for motion analysis to assess LW pieces and jams yielded a detection rate of 87 % in a Chilean river affected by a volcanic eruption and extensive riparian forest damage under minimal canopy cover (Sanhueza et al., 2019). A detection rate of 68 % was reported for LW counts along a river in western Michigan (USA) under open to moderate canopy cover (Gerke, 2019). Further, recall that the standing tree detection rate in this study was 98 %. In comparison, low to moderate canopy cover conditions yielded standing tree detections of 90 % accuracy for pine seedlings on farm and restoration sites in Australia (Finn et al., 2022), 85 % trees in a mixed conifer forest near Bridger-Teton National Forest, Wyoming (Mohan et al., 2017), and 72 % for living trees and 91 % for dead standing trees on a floodplain forest in northwest Portugal (Guerra-Hernández et al., 2021)

3.4. Channel hydraulics and hydrology

Peak discharges and stages for the April 2017 flood event were reconstructed for each sample reach using both the estimated 500-yr flood discharge reported generally for the region (Alexander and Wilson, 1995) and the HWM (high water mark) indicators surveyed during field work. Peak discharge estimates were calculated for each sample reach for a series of flood frequencies from the 2 to 500-yr events using published regional regression equations with input variables of drainage area and basin slope (Alexander and Wilson, 1995). Basin slope was calculated as the difference in elevation (rise) over the distance (run) using a 10 m DEM at points located at the 10 % and 85 % of the distance along the longitudinal profile of the main channel from the sample reach upstream to the drainage divide (Alexander and Wilson, 1995). The regional rating equation approach was used to provide an independent check on field-based measurements and to evaluate the reported flood frequency for the event for each site (Heimann et al., 2018).

Flood analyses based on HWM elevations were used to evaluate local variations in rainfall and flood routing on inundation depths and hydraulic variables. Valley floor cross sections were developed from auto-level surveys and analyzed using Intelisolve Hydraflow Express (2006) (Martin et al., 2021). Hydraulic parameters and discharge values were determined for bankfull stage and high-water mark elevations for each sample reach. In addition, stage-discharge relationships were developed for each site based on matching the hydraulic geometry of the valley to the predicted flood discharge values (Alexander and Wilson, 1995). Reconstructed flood stages were often >2–3 m higher than floodplain or terrace surfaces. Therefore, during hydrological calculations, Manning's n roughness coefficients were selected for different landform surfaces based on partial values from Chow (1959) to account for effects of substrate grain size and riparian forest density on flow as follows: 0.04–0.06 for channels/bars; 0.1–0.12 for floodplains and terraces; 0.04–0.10 for chutes; and 0.06–0.085 for valley floor features with significant riparian forest damage.

3.5. Hydrogeomorphic channel and floodplain analysis

Landform identification, classification, and mapping were accomplished using information from field mapping, DEM topography developed from SfM processing of UAV data, and hydrogeomorphic analysis. The March 2018 UAV imagery and GPS point location data for geomorphic features were used to create geomorphic maps and identify riparian forest damage in ArcMap. Aerial photographs and ArcGIS have been used before to assess forest damage (Kupfer et al., 2008; Getzin et al., 2012) and classify fluvial landforms (Dandois and Ellis, 2010; Watanabe and Kawahara, 2016). Using the UAV imagery and DEMs as a base map for field survey data, the locations of channels, floodplains, chutes, terraces, and tributaries were digitized (Fig. 2). Alluvial soil series data (USDA, 2005; USDA, 2006), DEMs/DSMs (Martin and Pavlowsky, 2011) and vegetation lines on streambanks (Vanlooy and Martin, 2005) were also used to identify landforms.

Hydrogeomorphic relationships were developed between calculated peak discharge and inundation frequency to identify the locations of channel, floodplain, and terrace features on the valley floor. Stage-discharge relationships were developed by slope-area methods using Intelisolve Hydraflow Express (2006) software to calculate channel hydrological and hydraulic variables for predicted discharges for different flood frequencies using regional equations by Alexander and Wilson (1995). Channel areas were defined as the horizontal area inundated by the predicted 1.5- to 2-yr recurrence interval flood. Field identification of bankfull stages typically matched those of the modeled channel. Floodplain features were identified by bank elevations above the bankfull channel extending to the valley margin or terrace banks features. Terrace features occurred at higher elevations than floodplains, usually at stages greater than the 5 to 10-yr recurrence interval flood. Chutes were mapped as secondary channels with bed elevations less

than the 2-yr flood stage. In this study, all features below bankfull stage in single and multithread channels including low bench, bar, and bed landforms were mapped individually and areas were combined to determine the total channel area for the sampling reach (Fig. 2). Therefore, the channel results of this study may not fully describe the geomorphic heterogeneity present below bankfull stage (Carling et al., 2014; Scott and Wohl, 2018).

Planform and stream power variables were determined for each sample reach. Sinuosity was calculated as the length of the channel along the thalweg divided by the straight-line distance between the start and end points of the reach (Leopold and Wolman, 1957; Brierley and Fryirs, 2005). Confinement ratio was calculated for each sample reach as the average of 11 transects of the width of the valley divided by the width of the bankfull channel (Nagel et al., 2014). Cross-sectional stream power and mean stream power were calculated for maximum flows at the predicted 500-yr flood discharge and median high-water mark (Bull, 1979; Lecce, 1997). Stream power describes the energy of the flow and the potential for geomorphic work. Large magnitude floods (>100-yr RI) can produce extremely high cross-sectional and mean stream power values in headwater channels thus increasing bank erosion and bedload transport rates (Bull, 1979; Müller, 1990; Costa and O'Connor, 1995; Lecce, 1997). Stream power affects the force of the water acting on the vegetation as well as the impact of sediment and debris encountering vegetation (Bendix, 1999). Mean stream power has been used before to evaluate the relationship between flood damage and riparian species distribution (Bendix, 1999).

4. Results and discussion

4.1. Channel and valley characteristics

The six stream reaches selected for assessment represent typical headwater streams for the Salem Plateau of the Ozarks Highlands including karst hydrology, channel form, sediment, and rural land use characteristics (Martin et al., 2021; Panfil and Jacobson, 2001). All six study watersheds drain 50 % or more forested land except Upper Tabor Creek, which drains only 42 % forest with 52 % in agricultural land (pasture and hay) and 5 % urban land (Table 1). Single-channel type streams were most common, but multithread channel types were present at upper Tabor Creek and Lick Branch (Lick Branch flows into the lower end of the upper Tabor Creek sample reach). The sample reach on Lick Branch drains only 4 km² and has the highest slope (0.15 m/m) among all sampling reaches. It lies in the transition zone between upland and lower gradient stream valley conditions with ephemeral hydrology, rocky valley floors, and relatively dense riparian forest stands. Karst geology creates losing channel conditions for several sample reaches where rapid subsurface drainage rates reduce baseflows to dry bed conditions for most of the year. Dry Creek, with the largest drainage area of 124 km², and Tabor Creek (both upper and lower reaches) were classified as losing channels by government agencies and were dry during field work visits except for one day after a rain (Table 1).

In general, LW deposition, in contrast to transport, is expected to increase in wider valleys with higher channel sinuosity, branching channel systems, lower banks, and relatively low slopes (Moulin et al., 2011; Polvi and Wohl, 2013; Ruiz-Villanueva et al., 2016a, 2016b). Indian Creek, lower Tabor Creek, and upper Tabor Creek have confinement ratios <3.8 (confined valleys) and therefore may be expected to provide LW for transport downstream in contrast to deposition (Nagel et al., 2014; Table 1). Streams in the Ozark Highlands in general tend to have lower reach sinuosity (<1.2) compared to other regions in the Midwest USA (Panfil and Jacobson, 2001). In this study, upper Tabor Creek is classified as a straight channel (sinuosity <1.06) and Dry Creek, Indian Creek, and Lick Branch are classified as low sinuosity channels (1.06–1.3) (Table 1). Sample reaches with higher sinuosity include Spring Branch (1.28) and lower Tabor Creek (1.7) with a sinuous channel (>1.3–3) (Brierley and Fryirs, 2005). Valley confinement does

not correlate with reach slope in this small sample of North Fork tributary sites. Reach slope tends to decrease with drainage area as expected (log-log, $p < 0.05$). However, Lower Tabor Creek and Dry Creek have relatively high slopes in comparison to drainage area. According to geologic maps, high reach slope (0.01) at lower Tabor Creek may be the result of geologic control by a monocline structure oriented across the valley.

The number (richness) and tendency for more equal distribution (diversity) of the four different landform types increased downstream with drainage area (Fig. 4). Lick Branch and upper Tabor Creek with multithread channels had a much greater proportion of the valley floor (about 60 %) covered by channel landforms including bed, bars, and lower benches as inclusively mapped here (Fig. 4). Three of the four reaches with single channels had intermediate channel areas covering 28 to 30 % of the valley floor. However, channel area for Spring Branch was relatively low (18 %), but with a relatively high terrace area (53 %) (Fig. 4). Excluding Lick Branch, percent terrace area of the reach tends to increase in wider valleys with higher confinement ratios (i.e., unconfined valleys) (Pearson $p < 0.1$). Single-channel types tended to have equal proportions of channel and floodplain areas, while the relative channel area in the two multithreaded channel reaches exceeded floodplain area by 1.5 to 1.7 times (Fig. 4). Chute development also increased downstream with drainage area from zero in the multithreaded reaches, 7 to 9 % in the middle reaches, and to 14 % at Dry Creek ($p < 0.02$) (Fig. 4). These trends are supported by previous work indicating that geomorphic complexity tends to increase downstream as valleys widen and develop greater topographic and hydrologic variability across the valley floor (Brierley and Fryirs, 2005).

Bankfull morphology was assessed for the post-flood channel by field surveys at each sample reach (Table 1). Topographic profiles of surveyed cross sections with high water marks are illustrated for all six reaches in Martin et al. (2021) with planform relationships detailed in Fig. 2 for this study. Relationships between drainage area and bankfull channel dimensions (i.e., width and mean depth) for North Fork tributary streams compare well with other regional datasets from Ozark Highlands streams (Martin et al., 2021). However, bankfull width and average depth values for the present study tended to be slightly larger than regional averages, suggesting that some degree of channel enlargement occurred during the 2017 flood leading to increased recruitment of LW for transport or redistribution to floodplain storages (Comiti et al., 2016; Martin et al., 2021). Average scaled bank height (i.e., average maximum field bank height/maximum bankfull stage) was < 1 at Lick Branch and Dry Creek, 1.1 at Spring Branch and Indian Creek,

1.2 at upper Tabor Creek, and 1.8 at lower Tabor Creek. Higher bank heights can confine LW to the channel for transport downstream rather than allow for deposition on banks and floodplains (Ruiz-Villanueva et al., 2016a, 2016b).

Median clast diameter for bed sediment (D50) ranged from 16 mm (coarse gravel) at Upper Tabor to 64 mm (very coarse gravel/fine cobble) at Lick Branch with size classifications after Rosgen (1996) (Table 1). The D50 was positively related to both reach and basin slope ($p < 0.01$), with a negative relationship to drainage area ($p < 0.05$). Average maximum clast size in the riffle crest did not correlate with slope or drainage area and ranged from medium cobble (108 mm) at Spring Branch to small boulder (512 mm) at Dry Creek (Rosgen, 1996). The study streams typically contained sub-reaches classified as mixed bedrock-alluvial channels with bedrock exposures often observed in deep pools, structurally controlled reaches, and along valley margins near steep rock bluffs (Panfil and Jacobson, 2001). Mixed alluvial-bedrock channels have been associated with relatively low to moderate sediment storage and LW loads (Welling et al., 2021).

4.2. Flood reconstruction

The Ozark Highlands produce some of the highest unit area discharge peaks in the USA because of high regional rainfall rates and relatively steep terrain (O'Connor and Costa, 2004). Recalling that the April 2017 flood was reported to be a > 500 -yr event (Heimann et al., 2018), estimated discharges for a 500-yr event had peak maximum depths ranging from 2.1 to 5.6 m that were 2.4 to 3 times higher than the maximum bankfull depth with mean velocities ranging from 1.5 m/s at Spring Branch to 2.4 m/s at lower Tabor Creek (Table 2) (Alexander and Wilson, 1995). Using field-based HWM indicators, peak flood heights ranged from 3.2 m at Lick Branch to 7.7 m at lower Tabor Creek and were 1 to 1.9-times deeper than the predicted 500-yr event. Flood reconstruction using HWMs at Lick Branch required some correction as described below. However, for the other five reaches, mean velocities ranged from 1.8 m/s at Indian Creek to 4.0 m/s at lower Tabor Creek and mean stream power ranged from 430 W/m² at Spring Branch to 1883 W/m² at lower Tabor Creek (Table 2).

Given the flashy hydrograph and large number of downed trees involved with the April 2017 flood event, it is expected that there would be large variability among at-a-site HWM elevations from tree scar, hanging debris, and strandline indicators. The HWM elevation was estimated as the average value of 4 to 10 HWM indicators at each surveyed cross section (Table 2; see Martin et al., 2021). Absolute

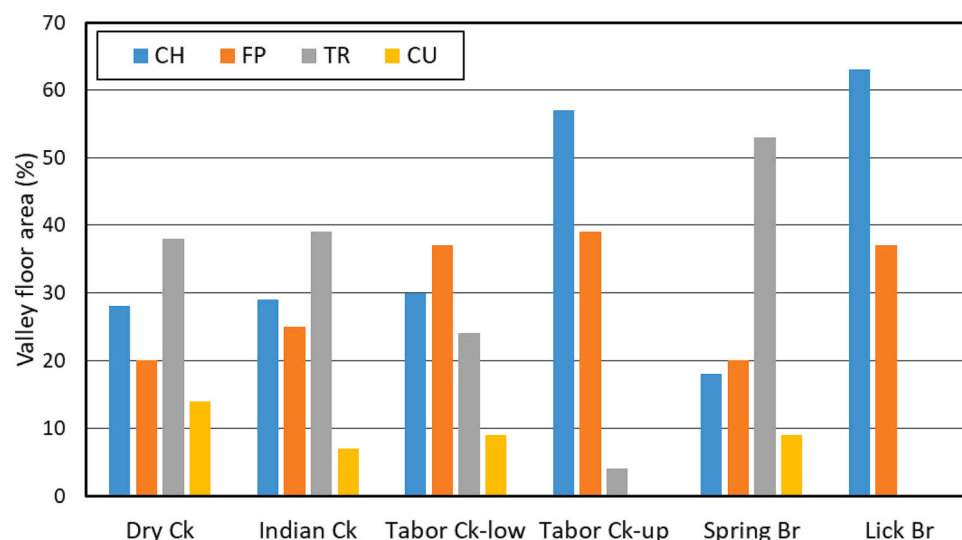


Fig. 4. Landform distribution by reach. Landforms as follows: CH, channel; FP, floodplain; TR, terrace; and CU, chute or secondary channel.

Table 2
Bankfull channel and 2017 flood characteristics.

Flood variable	Dry Creek	Indian Creek	Lower Tabor Creek	Upper Tabor Creek	Spring Branch	Lick Branch
Predicted 500-year flood						
Width (m)	117	124	97	81	131	26
Max Depth (m)	5.1	5.6	4.0	3.8	3.7	2.1
Relative depth (Flood/BF)	2.39	2.56	2.88	2.72	2.37	2.97
Velocity (avg., m/s)	2.12	1.80	2.40	2.09	1.50	2.02
Discharge (m ³ /s)	735	675	634	343	410	75.6
High water mark flood						
Width (m)	126	129	126	102	137	25
Max Depth (m)	7.3	5.6	7.7	6.7	4.6	3.2
Depth correction for Lick Br. (m)						1.6
Range in HWM heights (R, m)	1.2	2.4	3.3	6.0	2.9	1.5
HWM Samples (n)	7	10	5	6	10	4
HWM variability (%; 0.5 R/mean)	8	21	21	45	31	24
Relative depth (Flood/BF)	3.43	2.56	5.55	4.79	2.95	2.28
Velocity (avg., m/s)	2.88	1.76	4.04	3.32	1.91	1.74
Discharge (m ³ /s)	1708	657	2458	1557	790	46
Mean Stream Power (W/m ²)	780	467	1883	675	430	244
Total Stream Power (W/m)	100,773	45,076	241,146	76,503	64,406	5935

differences of site HWM elevations at one-half of the HWM range varied from 0.6 to 1.5 m with a median of 1.2 m among five sample reaches. However, the half-range value in upper Tabor Creek was 3 m where the valley was relatively narrow and tall trees were growing on the bed, bars, and benches of the multithread channel so that falling and floating trees could leave scars across a wide range of heights scattered about the peak flood stage. The relative variability of HWM elevations (1/2 range / mean in %) increases in the following order: 8 % at Dry Creek, 21 to 24 % at Indian Creek, lower Tabor, and Lick Branch, 31 % at Spring Branch, and 45 % at upper Tabor Creek (Table 2). Overall, the deepest, highest velocity, and most powerful floods occurred at the two Tabor Creek sites

(Table 2). Field inspections indicated the effects of deep and fast-moving flows in these two reaches including an approximately 6 Mg boulder resting on top of downed trees near transect 3 at lower Tabor Creek which was transported over 150 m downstream from a rock bluff during the flood (Fig. 2).

The HWM flood height for Lick Branch seemed somewhat unrealistic given a flood depth of 3.2 m for a watershed size of 4 km². Upon closer examination, backwater effects from the main channel of Tabor Creek were responsible for raising the water surface elevation by up to 3 m at the surveyed cross sections on Lick Branch. To correct the HWM flood stage at Lick Branch, a negative linear relationship was developed for

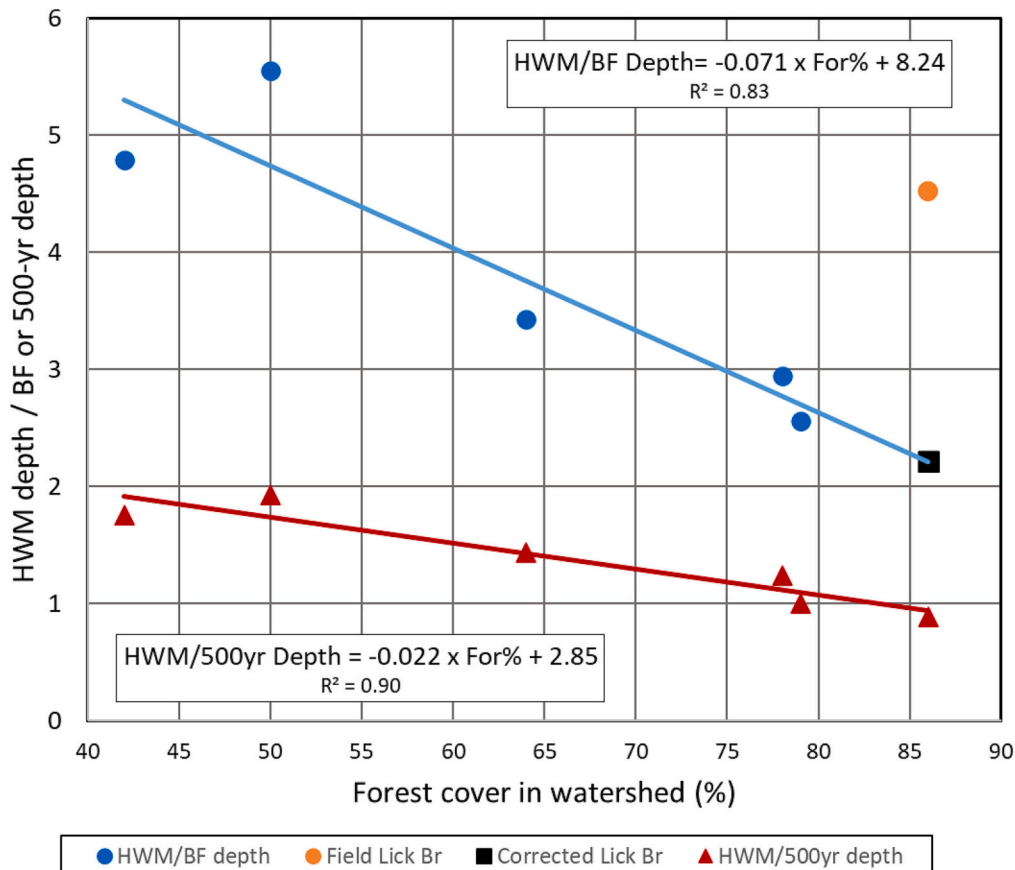


Fig. 5. Forest cover relationships with scaled depth ratios for 500-yr peak and 2017 HWM floods.

the other five reaches between percent of forest cover in the upstream watershed and the scaled maximum depth of the HWM flood calculated as the maximum depth of the HWM flood divided by the maximum depth of the bankfull stage ($p < 0.01$) (Table 2; Fig. 5). Using 86 % forest cover for Lick Branch watershed (Table 1) in the regression equation yielded a scaled HWM value of 2.21 that, when divided by a bankfull depth of 0.71 m, produced a corrected depth of 1.62 m for Lick Branch, about 1.6 m lower than the higher field estimate affected by backwater (Fig. 5). Scaled peak flood discharge, in addition to depth, also was inversely correlated with forest cover ($p < 0.01$) indicating that volume of flow from runoff was probably the main factor in depth control and not local hydraulic or geomorphic variables. Percent forest cover in the watershed was strongly related to scaled HWM flow variables but was not significantly ($p < 0.1$) correlated with drainage area, sinuosity, or valley width/confinement among the six samples reaches.

The relationship between forest cover and flood magnitude needs more work to verify since only six reaches were examined. Nevertheless, this finding suggests a combined anthropogenic influence of both land use (i.e., reduction in forest cover) and climate change (i.e., more intense rain events) on April 2017 flood magnitudes in the tributaries of the North Fork watershed. The sensitivity of flood magnitude to land use may be expected. During such an extreme rainfall event, soils become saturated and infiltration rates decrease to insignificant levels early in the storm after which the main control on runoff rates would be watershed roughness factors including higher depression storage and vegetation interception rates and lower drainage density and channel conveyance rates in forests compared to agricultural and urban areas (Eisenbies et al., 2007). This relationship is supported by predictions from rational runoff analysis of almost a doubling of the flood peak discharge for a 7.5 cm/day rainfall event between 85 % and 45 % forest cover in a small watershed (methods described in Ward and Trimble, 2003).

Forest cover seems to also influence water quality and possibly geomorphic stability in local streams. The lack of forest cover on uplands and along riparian corridors has been shown to increase runoff rates and pollutant loads in the Ozark Highland streams (Lopez et al., 2008). In addition, results from this study indicated a general tendency for both higher finer median sizes and larger maximum sizes of sediment on riffle beds in streams where forest cover was <65 % of the watershed area suggesting higher erosion rates during the flood in less forested watersheds. Indeed, Booth et al. (2002) suggested a threshold of 62 % to 74 % forest cover below which stream channels in rural areas may become

unstable with increasing bed and bank erosion rates.

4.3. Canopy loss by the flood

Large floods have the potential to cause riparian forest mortality both immediately during the flood by toppling, uprooting, and breakage and over the medium-term as damaged trees succumb to disease or weaken because of impact wounds or to substrate disturbance effects on roots (Palik et al., 1998; Acker et al., 2003). Except for Lick Branch where peak depth was <2 m, the 2017 flood inundated the entire valley floor of the sampling reaches to depths of 2 to 5 m over terrace surfaces (Table 2). At these flow depths, and with some average flow velocities >3 m/s, extensive damage to riparian trees may be expected. Acute forest mortality was assessed for the 2017 flood by evaluating the area percent of riparian canopy loss during the flood (Fig. 6). Canopy cover before the flood (2016) was as follows: Dry Creek, 94 %; Indian Creek, 81 %; Lower Tabor Creek, 99 %, Upper Tabor Creek, 100 %; Spring Branch, 89 %; and Lick Branch, 100 %. At the reach scale, flood-induced canopy loss was greatest at Lower Tabor Creek (63 %) with highest slope and sinuosity and lowest at Spring Branch (12 %) and Indian Creek (14 %) with relatively wide valleys. Dry Creek had relatively high canopy loss, twice as high as the other single-channel reaches besides lower Tabor Creek. Both reaches with relatively high canopy loss had relatively high channel slopes given their location in the watershed (Fig. 6).

Cross-sectional and mean stream power was highly correlated with canopy loss ($p < 0.01$). To a lesser degree, flood depth ($p < 0.05$) and relatively narrow valleys ($p < 0.1$) were also related to canopy loss. Among landforms, canopy loss was 79 % in the channel at lower Tabor Creek but was much less than that, from 19 to 32 %, at the other sample reaches (Fig. 6). Floodplains and to a lesser degree terraces and chutes tended to have higher canopy loss rates in downstream reaches. But overall, lower Tabor Creek had canopy loss rates for all landforms, except terraces, that were two to three times greater than the other sample reaches (Fig. 6). Again, these findings underscore the roles of flood depth and valley morphology to enhance or diminish the effects of large floods on forest damage and LW recruitment (Palik et al., 1998; Ruiz-Villanueva et al., 2016a, 2016b, 2018).

4.4. Post-flood standing tree density

In total, 1214 standing trees were assessed from UAV imagery by this study (Fig. 2). Ground-truthing indicated that STD was accurately

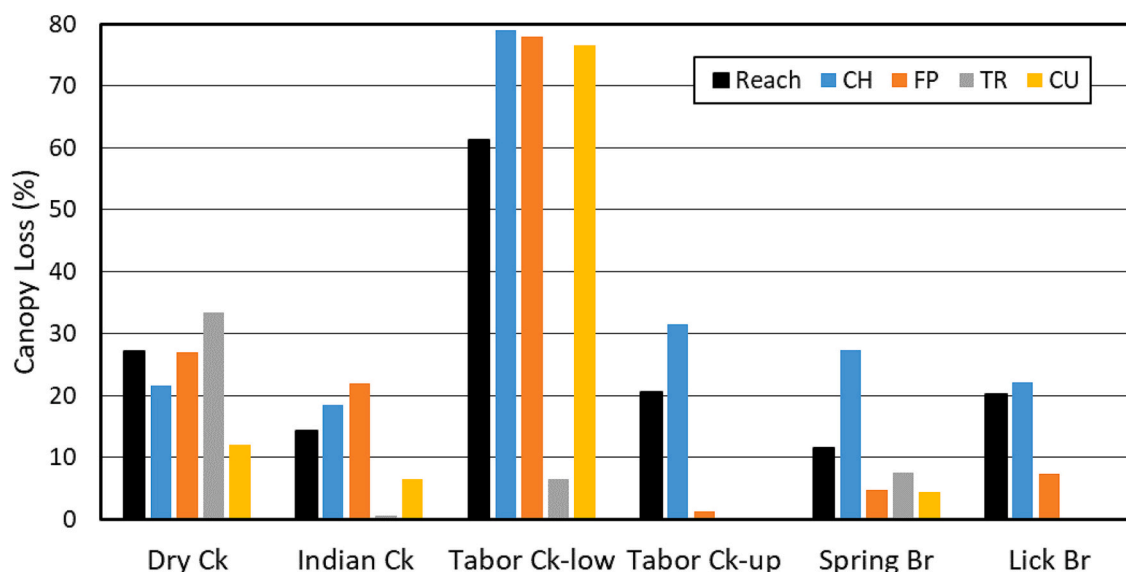


Fig. 6. Tree canopy loss by reach and landform. Landforms as follows: CH, channel; FP, floodplain; TR, terrace; and CU, chute or secondary channel.

measured from UAV imagery and no corrections were needed. Note that STD values from UAV data were typically <150 trees/ha among landforms as well as sampling reaches overall (Table 3A). By reach, STD generally increased in the order: 50 trees/ha for lower Tabor Creek and Indian Creek; 75 trees/ha for Spring Branch and upper Tabor Creek; 125 tree/ha for Dry Creek; and 240 tree/ha for Lick Branch (Table 3A). Except for the two multithread reaches, lowest STD occurred in channel areas, while the highest values were found on floodplains and terraces (Fig. 7). Lick Branch reach has an overall STD of almost 250 tree/ha reflecting its transitional location between upland and riparian forest conditions. These values may be lower compared to upland forests but fall within the range reported for oak-pine forests in the Ozark Highlands of 130–318 trees/ha with an average of 247 trees/ha (Hanberry et al., 2014). Compared to upland forests, valley floor STD was probably reduced by naturally lower STD in open canopy channel bed and bar areas and tree mortality caused by the 2017 flood (Fig. 6). Riparian forests affected by frequent or higher energy floods tend to have lower tree densities, particularly of younger trees, compared to upland forest forests affected by similar climate and geology (Palik et al., 1998; Garssen et al., 2015; Saint-Laurent et al., 2019).

4.5. Number, size, and alignment of LW pieces

In total, 1560 downed wood pieces (corrected from 1013 pieces from raw UAV analysis) were assessed by this study (Fig. 2). By reach, the two multithreaded reaches contained the highest number of LW pieces in the channel (about 70 %) (Fig. 8). In contrast, single channel reaches only contained 8–24 % of total LW pieces in the channel, slightly below the distribution of channel area within reaches of 18–30 % (Fig. 3). The importance of chutes as locations for deposition of LW increases downstream from 6 % of the total number of pieces at Spring Branch with a drainage area of 49 km² to 20 % at Dry Creek with a drainage area of 124 km², probably related to the general trend of valley widening and increased landform diversity downstream (Table 1; Fig. 4). No chutes

Table 3
Standing tree density and large wood loads by reach and landform.

Reach	CH	FP	TR	CU	Total
A) Standing tree densities from UAV imagery (#/ha)					
Dry Ck	87	129	163	105	127
Indian Ck	10	53	79	32	50
Tabor Ck-low	25	37	114	39	52
Tabor Ck-up	68	108	50		83
Spring Br	25	102	96	85	77
Lick Br	265	207			243
B) Large wood loads from UAV imagery (m ³ /ha)					
Dry Ck	11.4	33.6	31.2	40.7	27.4
Indian Ck	15.9	35.3	14.8	29.6	21.3
Tabor Ck-low	24.8	28.0	15.5	21.5	23.4
Tabor Ck-up	25.8	4.3	19.7		17.2
Spring Br	17.4	4.2	11.0	4.6	10.2
Lick Br	5.6	4.5			5.2
C) Large wood loads- corrected (m ³ /ha)					
Dry Ck	16.0	55.0	56.9	61.5	44.6
Indian Ck	15.7	43.1	20.2	32.8	25.6
Tabor Ck-low	26.4	31.6	24.2	24.6	28.5
Tabor Ck-up	33.7	6.6	23.8		23.9
Spring Br	18.6	6.3	16.1	6.5	13.9
Lick Br	13.3	9.3			11.8
D) Large wood distribution by volume- corrected (% of reach)					
Dry Ck	9.8	24.1	47.3	18.8	100
Indian Ck	17.9	42.2	30.9	9.0	100
Tabor Ck-low	28.7	42.3	21.0	8.0	100
Tabor Ck-up	84.5	11.3	4.2		100
Spring Br	24.4	9.2	62.2	4.2	100
Lick Br	70.9	29.1			100

were mapped in the multithread reaches (Fig. 7). However, it is important to note that after the 2017 flood, more than two-thirds of the LW pieces were deposited at relatively high elevations and distal locations on floodplains and terraces in single channel reaches (Fig. 7) (Ruiz-Villanueva et al., 2016a, 2016b). Moreover, more than half of the individual pieces of LW were found on terraces in the sample reaches at Spring Branch and Dry Creek (Fig. 7). Overall, single-channel reaches stored >3 times more wood pieces in floodplain and terrace areas compared to channel areas.

The size of LW pieces compared to channel width or flood depth can indicate the relative importance of transport or storage in a reach where relatively smaller pieces are transported downstream or laterally more easily (Gurnell et al., 2002; Scott and Wohl, 2018; Ruiz-Villanueva et al., 2016a, 2016b). Large wood diameter in the channel averaged 10 to 23 cm among reaches with 95 %-tile values from 19 to 44 cm. As discussed above, piece length tends to be underestimated by measurements from UAV imagery. However, with this limitation in mind, some observations relevant to wood transport are described. Large wood length in the channel decreased among sites in the order: Spring Branch and Indian Creek (12 m); Upper Tabor Creek, Lower Tabor, and Dry Creek (8 m); and Lick Branch (5 m) with 95 %-tile values decreasing in the order: Indian Creek (20 m); Spring Branch, upper and lower Tabor Creek, and Dry Creek (15 m), and Lick Branch (9 m). Both Spring Branch and Indian Creek had relatively high STD on terraces and floodplains compared to the other reaches (Table 3A). Among reaches, the mean LW length in the channel was positively related to mean LW length in floodplains ($p < 0.05$) and chutes ($p < 0.05$). In addition, mean length of LW by reach was positively related to percent terrace area (<0.02) and negatively related to percent channel area ($p < 0.02$). This suggests that the supply of larger trees to the channel may have originated from higher elevation substrates supporting older stands that are less frequently affected by flooding, but possibly more susceptible to damage by larger floods (Lyon and Sagers, 1998; Swanson et al., 1998; Fierke and Kauffman, 2006; Fischer et al., 2021; Huylenbroeck et al., 2021).

Mobility ratios calculated as mean LW length divided by mean bankfull width were much lower than one (i.e., <0.45) for all reaches and landforms suggesting that wood recruited from those sites or upstream may tend to be transported downstream rather than deposited and stored locally (Fig. 8) (Gurnell et al., 2002; Martin et al., 2021). Interestingly, both Tabor Creek reaches had the highest mobilities (lowest ratios <0.23). Field observations may support this, since several large jams containing multiple downed mature trees were observed below these sampling reaches. Nevertheless, given the relatively wide channels for all sample reaches, the tendency would be for downstream transportation of free or floating LW, rather than storage in the channel, in the North Fork tributaries studied here (Martin et al., 2021).

Large floods that generate fast and deep currents will impact trees with hydraulic force or floating wood that can topple standing trees or bury downed trees with eroded sediment (Johnson et al., 2000; Guiney and Lininger, 2021). As an indicator of hydraulic and impact effects, LW orientation was frequently (>50 %) aligned parallel to flow direction in the main channel or adjacent chutes (Figs. 2 & 9). Lick Branch, Spring Branch, and Indian Creek with mean stream powers <500 W/m² had lower percentages of aligned wood pieces by reach (57 to 68 %) compared to lower and upper Tabor Creek and Dry Creek having mean stream power values >500 W/m² with higher frequencies of aligned wood (87 to 96 %) (Table 2, Fig. 9). Typically, terraces had the lowest percent flow-aligned pieces among landforms varying from 45 to 53 % for Spring Branch, upper Tabor Creek, and Indian Creek to 85–94 % at lower Tabor and Dry Creeks (Fig. 9). Trees growing on terraces were usually, but not always, farther away from the channel so that direct contact with strong currents and falling trees was limited causing the supply rate of floating wood to increase over that of flow-aligned toppled trees.

Percent aligned LW increased with HWM flood peak discharge and depth (<0.01), scaled HWM flood depth ($p, <0.05$), and cross-sectional

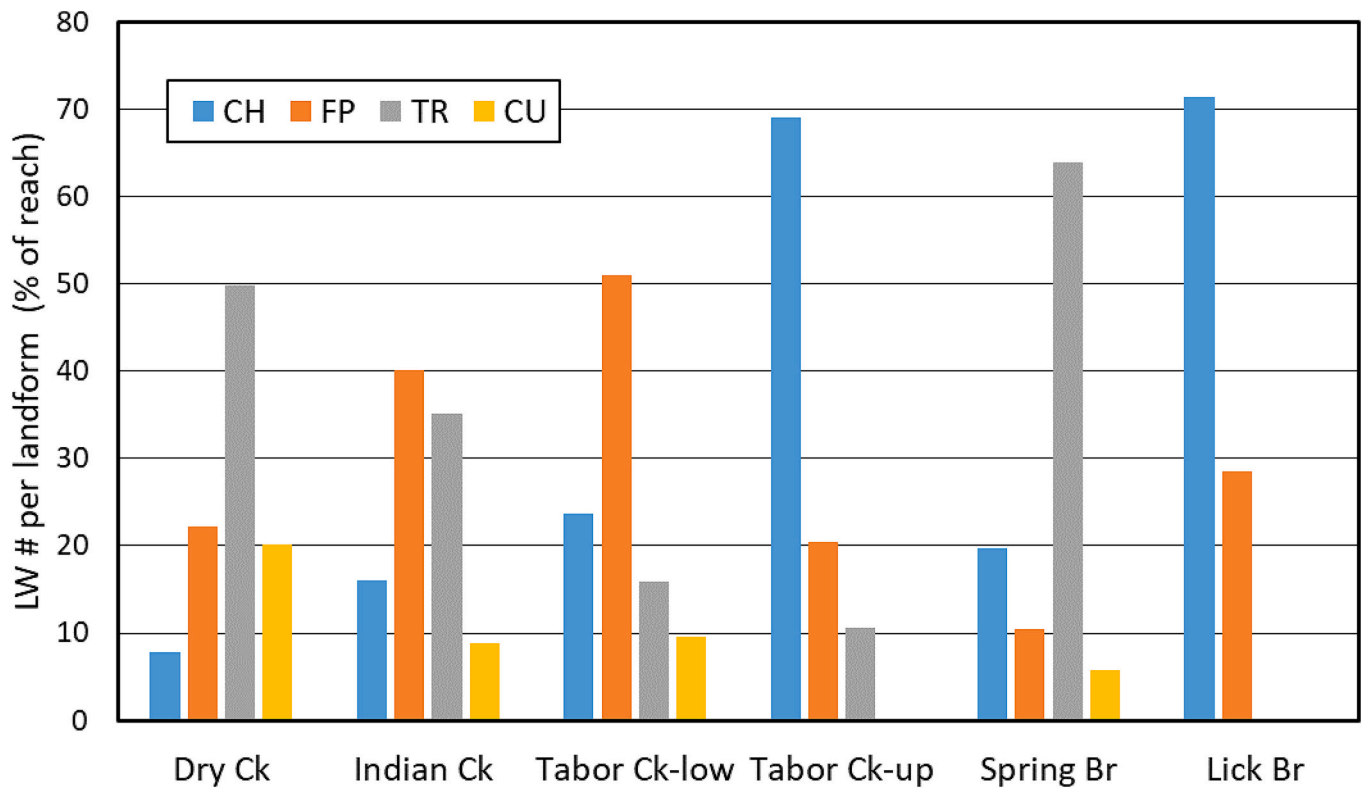


Fig. 7. Distribution of LW pieces by landform. Landforms as follows: CH, channel; FP, floodplain; TR, terrace; and CU, chute or secondary channel.

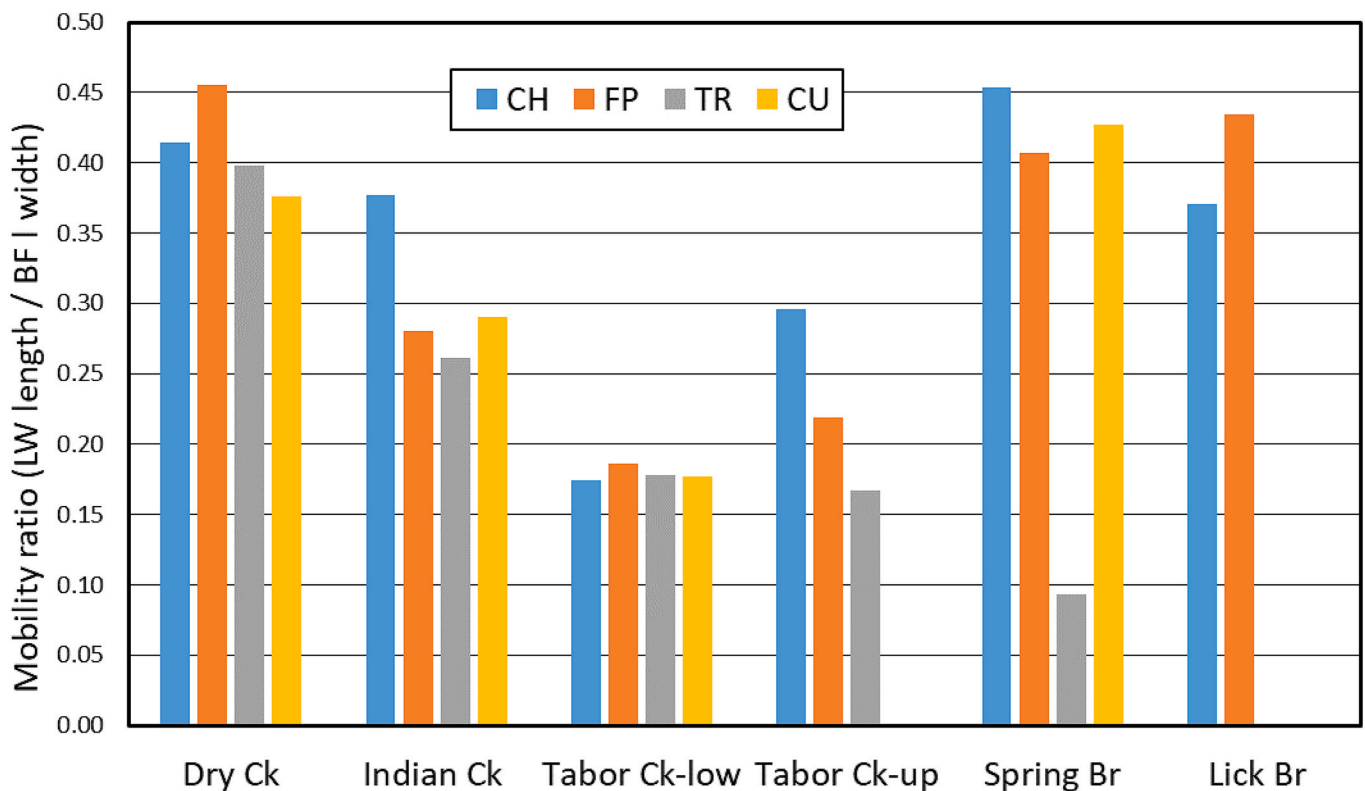


Fig. 8. Mobility of large wood. Landforms as follows: CH, channel; FP, floodplain; TR, terrace; and CU, chute or secondary channel.

and mean stream power (P , <0.1), but not confinement ratio, suggesting that flood power was the main variable influencing LW alignment, similar to tree damage indicated by canopy loss (Fig. 6). Field

observations at sampling reaches indicated a high frequency of toppled trees, many still partially anchored by roots (Fig. 3). Therefore, tree toppling with remaining root anchoring during the flood probably

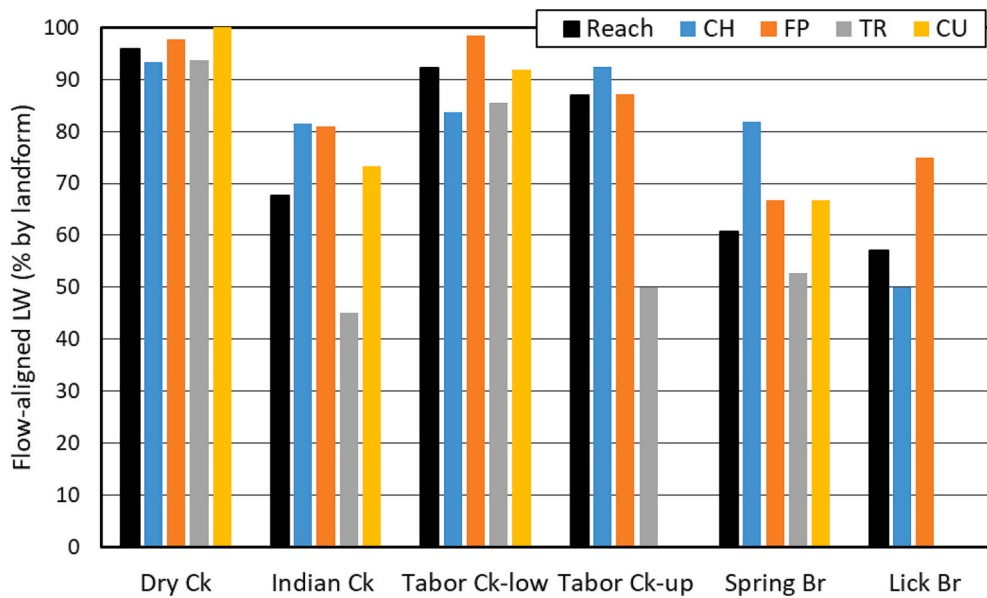


Fig. 9. Flow alignment of large wood. Landforms as follows: CH, channel; FP, floodplain; TR, terrace; and CU, chute or secondary channel.

accounted for the high degree of flow alignment by LW since downed trees could not float freely or be transported far from original growing location and thus were susceptible to flow alignment and partial burial of the upstream root wad end of the downed tree.

4.6. Distribution and frequency of jams

The presence of jams indicates that some degree of LW transport has occurred during a flood (Wohl and Jaeger, 2009; Atha and Dietrich, 2016). Jams in the western USA may be expected to store the largest volume of LW in medium rivers in channels 20–50 m wide (Kramer and Wohl, 2017). However, this was not the case in the North Fork tributaries after the 2017 flood (Martin et al., 2021). We identified 24 jams in UAV imagery within the six reaches with only one at Lick Branch; four at Spring Branch, lower Tabor Creek, and Dry Creek; five at Indian Creek; and six at upper Tabor Creek (Table 4 and Fig. 2). Jams contained an average of 3.3 to 5.3 pieces by reach (Table 5). Jam density increased among reaches from 1/ha at Spring Branch and lower Tabor Creek, 1.5/ha at Indian Creek, 2/ha at Dry Creek, 2.5/ha at upper Tabor Creek, and 3/ha at Lick Branch, with highest density in the multithreaded reaches. Jam density generally increased in reaches with higher STD ($p < 0.02$), lower average bank height ($p < 0.02$), and lower sinuosity channels ($p < 0.1$). In the western USA, deeper and multithreaded channels tended to store more LW in jams compared to other channel types (Scott and Wohl, 2018). However, this trend was not clear in this study. The percentages of LW pieces in jams increased among sample reaches as follows: 5–10% for upper and lower Tabor Creeks and Dry Creek; 15% for Indian Creek; and 23–29% for Lick Branch and Spring Branch. The percentage of wood pieces deposited in jams was negatively related to drainage area ($p < 0.05$), scaled HWM depth (<0.02), and mean stream power ($p <$

Table 4
Jam distribution.

Reach	Jam Count		Jams per landform (%)				% in CH+ 10 m buffer
	#	#/ha	CH	FP	TR	CU	
Dry Ck	4	1.9	25	25	50		50
Indian Ck	6	1.5	33	17	50		50
Tabor Ck-low	4	0.8	75		25		100
Tabor Ck-up	5	2.5	80		20		100
Spring Br	4	1.2	25		75		50
Lick Br	1	3.3	100				100

Table 5
Relationships between large wood loads and hydro-geomorphic variables.

Variable	Load Value*	Channel [#]	Flood plain	Terrace	Chute	Reach
Drainage Area	Cor	-0.07	0.88	<u>0.77</u>	0.94	0.87
	UAV	0.14	0.84	<u>0.71</u>	0.96	0.90
Sinuosity	Cor	0.21	0.10	-0.27	-0.46	0.03
	UAV	0.45	0.26	-0.41	-0.40	0.25
Bed slope	Cor	-0.23	-0.18	0.36	0.23	-0.23
	UAV	-0.47	-0.23	0.30	0.20	-0.39
Confinement Ratio	Cor	-0.76	0.14	0.48	0.24	0.04
	UAV	-0.76	-0.05	0.32	0.02	-0.22
Scaled flood depth	Cor	0.86	0.00	-0.02	-0.04	0.34
	UAV	0.84	0.09	0.06	-0.02	0.48
Total stream power	Cor	0.49	0.30	0.08	-0.02	0.44
Mean stream power	UAV	0.63	0.41	0.01	0.01	0.60
	Cor	0.49	0.30	0.07	0.02	0.42
	UAV	0.61	0.42	0.02	0.07	0.59

* Cor, corrected UAV loads based on STD calibration; UAV, initial results from imagery analysis.

[#] p values. Underlined values are significant at $p < 0.05$ and bold values at $p < 0.02$.

0.05). This trend possibly indicates that jams were relatively more important LW storages in reaches affected by lower flood magnitude flood since lower rates of tree toppling did not contribute as much wood to assessed loads in addition to the transported wood in jams.

Jam deposition tended to decrease with distance away from the channel because of lower flow velocities and depths in interior floodplain areas, trapping of LW by trees as obstacles to wood transport, and shorter durations of inundation or wood supply on higher landforms (Ruiz-Villanueva et al., 2016a, 2016b; Lininger et al., 2021; Guiney and Lininger, 2021). Patterns of jam formation become clearer with Lick Branch being excluded from evaluation with only one jam and being affected by other confounding factors such as smallest drainage area, backwater influence, and lowest scaled flood depth. The relative percent of total jams in the channel was strongly correlated with scaled flood depth ($p < 0.01$) where reaches having lower scaled flood depths <3.5 contained $<30\%$ of total jams in the channel (Fig. 2). The highest percentage of jams occurred in channels with the highest scaled flood

depth at upper (80 %) and lower (75 %) Tabor Creek reaches (Table 4). In general, from 50 to 100 % of jams were deposited within a 10 m distance extending out across the valley floor from the bank lines of the channel. While not a significant predictor for jam density in this study, there was a tendency for reaches with relatively wider valleys to have lower percentages of jams in the channel (Guiney and Lininger, 2021). Larger floods may be expected to produce more jams in the channel (Guiney and Lininger, 2021). Nevertheless, in reaches where the confinement ratio was >3 (relatively unconfined), 50–75 % of the jams were located on in terraces indicating that floods can move significant loads of LW into storage and form jams in distal valley floor areas along Ozark Highland streams (Table 4) (Wohl et al., 2018).

4.7. Large wood loads (m³/ha)

The distribution patterns of LW loads in the North Fork tributaries generally followed trends described in previous studies (Fig. 2). Large wood storage sites in the sampling reaches occurred along: (i) higher bank lines at channel margins, (ii) bends on outer banks and inner point bars in contrast to straight reaches, and (iii) heads or edges of islands or secondary channels often where a chute or secondary channel diverges from the main channel (Nakamura and Swanson, 1994; Johnson et al., 2000; Gurnell et al., 2002; Ruiz-Villanueva et al., 2016a, 2016b; Guiney and Lininger, 2021). Channel bends allow overbank flows to directly enter riparian forests, maximize bank erosion rates, increase the supply of floating or downed wood for collisions, and enhance wood deposition (Leopold and Wolman, 1957; Murphy and Koski, 1989; Nakamura and Swanson, 1994; Hupp and Osterkamp, 1996; Piégay and Marston, 1998; Johnson et al., 2000; Gurnell et al., 2002; Hupp and Bornette, 2005; Fuller, 2007). At Spring Branch, Indian Creek, and Dry Creek, clusters of deposited floating and aligned wood were found tens of meters away from the channel below riffles and bar heads on floodplains and terraces with nearby chutes along the valley margin (Fig. 2).

Corrected LW loads tended to exhibit the same general trends as observed for the raw UAV LW loads (Table 3B & C). Paired values of corrected and UAV LW loads are strongly correlated ($p < 0.01$) with reaches with the highest STD indicating the largest increases in load estimates at Lick Branch (2.3 times) and Dry Creek base (1.6 times) with corrections for the other reaches ranging from 1.2 to 1.4 times UAV

loads. Corrected LW loads by reach increase downstream with drainage area ($p < 0.01$) being highest at Dry Creek (45 m³/ha), moderate at upper (24 m³/ha) and lower (29 m³/ha) Tabor Creek and Indian Creek (26 m³/ha), and lowest at Lick Branch (12 m³/ha) and Spring Branch (14 m³/ha) (Table 3C). Channel LW loads were highest at lower (26 m³/ha) and upper (34 m³/ha) Tabor Creek with loads decreasing by half to 13–19 m³/ha in the other four reaches (Fig. 10). Floodplain loads tended to be <10 m³/ha for watershed areas <60 km² but increased downstream to a maximum of 55 m³/ha at Dry Creek draining 124 km². Chutes responded similarly to floodplains, with LW loads increasing downstream from 7 m³/ha at Spring Branch to 62 m³/ha at Dry Creek. Terrace LW loads ranged from 16 to 24 m³/ha for the five reaches draining watershed areas <102 km², but approximately tripled to 57 m³/ha at Dry Creek with the largest drainage area (Table 1 and Fig. 10). Recall that the percent of total LW volume (m³) within the reach stored by a landform generally follows land area trends (Table 3D and Fig. 4). While multithread reaches store >70 % of LW volume in the channel, single-channel reaches only store 10–30 % of LW volume in the channel. Valley floor features contain the largest volumes of LW with up to 42 % on floodplains, 62 % on terraces, and 19 % in chutes (Table 3D).

Large wood deposition is often concentrated in the near-channel area since wood supplies can enter a reach via the channel from upstream sources, shallowing flows along channel banks can strand wood, and channel widening during a flood will focus wood recruitment and deposition along channel banks (Ruiz-Villanueva et al., 2016a, 2016b). As defined here, the near-channel area consists of the previously defined channel area added to the area of a 10 m buffer extending outward from each bank (Fig. 2). Near-channel area as the percent of total reach area increases in the following order among sample reaches: Spring Creek, 34 %; lower Tabor Creek, Indian Creek, and Dry Creek, 50 %; upper Tabor Creek, 82 % and Lick Branch, 100 %, and with the highest values in the multithreaded reaches. The percentage of LW load deposited within the near-reach zone in each reach was lowest at Dry Creek (30 %) and Spring Branch (44 %), moderate at Indian Creek (53 %) and lower Tabor Creek (55 %), and highest at Lick Branch (85 %) and upper Tabor Creek (96 %). Again, the distribution of near-channel LW emphasizes the differences between single-channel and multithread reaches in LW processing and the importance of LW recruitment and storage on floodplains and terraces typically at volumes of half or more of the total

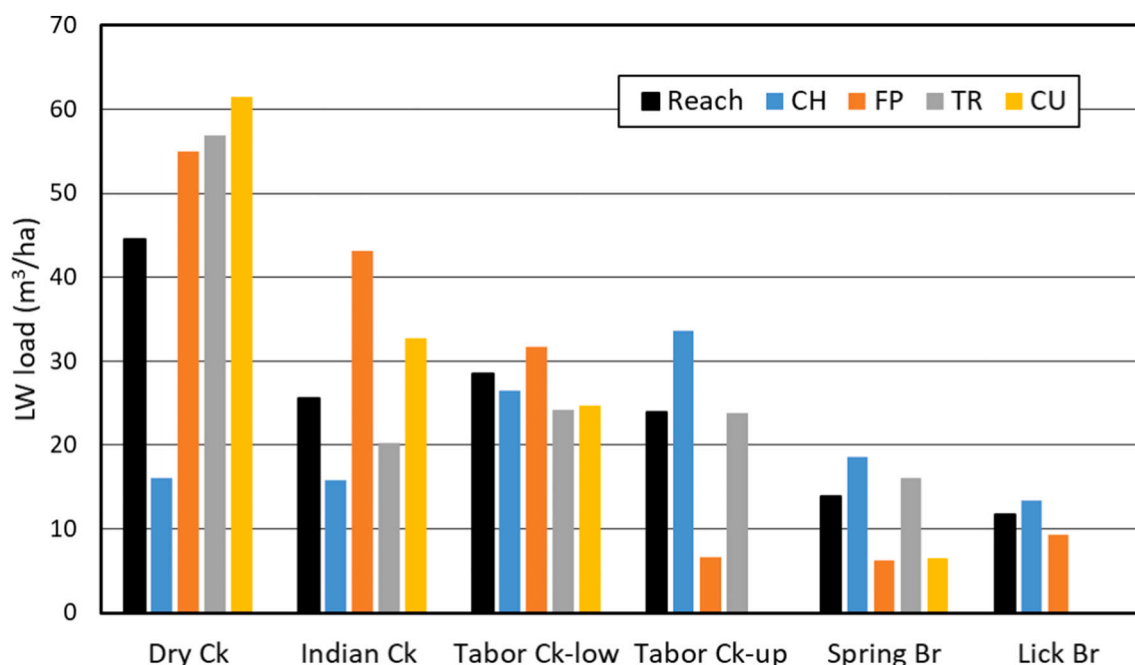


Fig. 10. Corrected large wood loads by landform. Landforms as follows: CH, channel; FP, floodplain; TR, terrace; and CU, chute or secondary channel.

LW load stored in the reach.

Previous studies indicated that LW loads in the channel typically decrease downstream because of increased mobility for transport downstream or out of the channel by overbank flows or chutes and lower slopes, flood power, and recruitment rates over all (Wohl and Jaeger, 2009; Comiti et al., 2016; Ruiz-Villanueva et al., 2016a, 2016b). In the present study, LW loads in the channel showed no relationship with drainage area (Table 3). Moreover, LW loads in the channel were positively related to relatively narrow valleys ($p < 0.05$) and scaled flood depth ($p < 0.02$) suggesting that deeper floods can recruit more wood for channel deposition or toppling if wider valley floors are not available for wood storage or flood attenuation. Positive relationships with drainage area by LW loads were also observed for floodplains ($p < 0.01$), terraces ($p < 0.05$), and chutes ($p < 0.01$) (Table 5 and Fig. 10). As expected, LW loads in chutes also increased downstream in relatively wider valleys ($p < 0.02$ with confinement ratio). Interestingly, LW volumes in the extended near-channel area were positively related to drainage area ($p < 0.05$). The lack of correlation of drainage area with channel loads compared to its significance for near-channel loads suggests that LW recruitment and storage can fluctuate over short distances along channel margins during large floods.

Using field methods and not UAV data collection, Martin et al. (2021) reported LW loads for the same channel reaches used in this study. The loads from Martin et al. (2021) typically fell in the range between the UAV and corrected LW loads. However, the channel loads by Martin et al. (2021) for Spring Branch and Indian Creek were $> 40\%$ higher than those from the present study. Compared to the other reaches, these sample reaches had relatively large LW loads on floodplain and terrace areas immediately adjacent to or sometimes overlapping into the channel. Therefore, compared to the present study, Martin et al. (2021) probably included additional LW pieces from the floodplain and terrace margins in their channel load estimates. This comparison underscores the importance for understanding how differences in sampling procedures can affect the results and measurement errors in LW assessments (Kaufmann et al., 1999; Wohl et al., 2010).

4.8. Downstream LW transport models

The results of this study provide insights into downstream relationships among recruitment, transport, and deposition of LW in channels or on floodplains in these forested watersheds. As headwater drainages in the North Fork watershed transition from colluvial to fluvial channel systems, wood mobility is transport-limited because of shallow flows and narrow/rough channel (Marcus et al., 2002; Gurnell et al., 2002; Wohl et al., 2018). Albeit with only one site to assess, a flood depth threshold of about 2.5 times the maximum bankfull depth may need to be exceeded before currents and floating wood can sufficiently impact riparian trees, overwhelm substrate roughness and strength, and cause toppling or uprooting of standing trees on floodplains and terraces. Lick Branch with a small drainage area (4 km^2) sustained relatively low rates of canopy loss and LW loads in comparison other sites farther downstream while having the highest bed slope (0.015) and standing tree density (Figs. 6 & 10). Geomorphic stability of Lick Branch was also inferred since it was a multithreaded channel with intact root mat, low shrub cover, and exposures of boulders/bedrock on the bed. While not assessed for this study, two other nearby tributary reaches draining $< 10 \text{ km}^2$ also exhibited very little tree damage and low LW loads even though road bridges were washed out $< 500 \text{ m}$ downstream.

As drainage area increases from 10 km^2 to $> 100 \text{ km}^2$, LW loads in the channel tend to fluctuate downstream between 13 and $19 \text{ m}^3/\text{ha}$ with higher loads of $26\text{--}34 \text{ m}^3/\text{ha}$ at the two Tabor Creek reaches possibly caused by higher flood peaks, confined valleys, and locally higher channel slopes (Tables 1 & 2) (Swanson et al., 1998; Johnson et al., 2000). Other workers have found that LW loads in the channel tend to decrease by unit distance, landform area, or drainage area (e.g., Marcus et al., 2002; Wohl and Jaeger, 2009; Comiti et al., 2016). While the

sample size in this study limited the in-depth analysis, we found no significant trend between drainage area and channel LW loads. However, channel load per unit drainage area did significantly decrease downstream with a best-fit power function with an r^2 value of 0.98 including all six sites and 0.67 excluding Lick Branch.

In contrast to the channel, LW loads increased downstream with drainage area on floodplains ($p < 0.01$), terraces ($p < 0.05$), and in chutes ($p < 0.01$). Large wood loads increased on floodplains from 6 to $16 \text{ m}^3/\text{ha}$ at Spring Branch (49 km^2) to $55\text{--}62 \text{ m}^3/\text{ha}$ at Dry Creek (124 km^2) as the storage capacity across the valley floor increased because of valley widening, increased frequency of chutes, and possibly relatively lower bank heights (Ruiz-Villanueva et al., 2018; Wohl et al., 2018). Large wood loads per unit drainage area were weakly related to drainage area for floodplains and terraces but showed a positive relationship for chutes ($p < 0.05$). While in some watersheds, channel LW loads were greater than floodplain loads (Lininger et al., 2017), the present study found that floodplains stored more LW per unit area than the channel as drainage area increased beyond 50 km^2 (Table 4). Further, excluding the two multithread reaches where channels stored 71–85 % of the total LW volume, $> 70\%$ of the total volume of LW storage in the reach was on floodplains, terraces, and chutes (Table 3D). Martin et al. (2021) found that channel loads in these North Fork watersheds were like those measured in other rivers in the Ozarks not affected by recent large floods. This study indicates that channel loads were variable downstream at low to moderate levels. However, LW loads increased dramatically downstream on floodplains, terraces, and in chutes. Thus, floodplains are providing important storages and riparian source areas for LW in the Ozarks Highlands.

The degree to which the stored LW by the 2017 flood will be remobilized from channel and floodplain locations and be made available for geomorphic and habitat functions is unclear. Field surveys in the channel after the flood indicated that new wood represented from 5 to 35 % of pieces at these sites and that a higher proportion of pieces had attached root wads compared to other streams in the Ozarks not affected by a large flood (Martin et al., 2021). While not evaluated for this study, if flow aligned wood on floodplains is an indicator of the distribution of downed trees with roots attached then up to 50–90 % of LW pieces by reach could have still been anchored in place after the flood (Fig. 9). The removal of LW from floodplains can occur in four ways: (i) fluvial transport by floating and hydraulic force; (ii) burial by channel or floodplain sediment, (iii) wood decay and break up into smaller pieces; and (iv) direct removal by human actions or possibly beaver use (Wohl, 2013; Pollock et al., 2014; Lininger et al., 2017).

The time until the occurrence of a flood stage deep enough to float large wood on terraces is generally unpredictable. But the 2017 “storage event” was an infrequent occurrence that even with climate change influence may not occur again for a long period (Heimann et al., 2018). Further, attached root wads limit the rate of initial mobilization and travel distance (Kramer and Wohl, 2017). While oak logs 14,000 yr old were found buried under floodplain deposits in northern Missouri with a glacial history (Guyette et al., 2008), wood preservation under the climate and sedimentation conditions in Ozark streams are limited with intact buried wood being a rare find. Thus, decay and breakage may be the primary process by which the recently stored wood is ecologically processed. Deciduous log residence times under these climate conditions are typically $< 15 \text{ yr}$ while conifers typically range from 20 to 80 yr or longer (Ruiz-Villanueva et al., 2016a, 2016b). Additional monitoring to determine the fate of the stored wood in the channel and floodplains can help to better understand how flood-stored LW is cycled in this region. However, field observations indicated that downed wood on floodplains can break up and decompose to lose its structural integrity in 5–10 yr in the North Fork watershed.

5. Conclusions

With increasing concerns of larger more frequent floods, a better

understanding of the interaction among fluvial processes, riparian forest damage, and LW loads can result in improved preparedness and responses to climate change. Few studies have been completed on the relationships among drainage area, valley morphology, and LW loads in the channel and on floodplains in the Midwest region (Cordova et al., 2007; Martin et al., 2018, 2021). This work provides much needed data on the relationship between large flood effects on riparian forests and the recruitment of LW in the Ozark Highlands. One of the drawbacks of this study is that only six sites were sampled. Nevertheless, 1214 standing trees and 1013 LW pieces were assessed on four different valley floor landforms, which addresses a significant gap in our knowledge of flood-related LW recruitment and storage in fluvial systems (Wohl, 2017; Lininger et al., 2017). In addition, the use of UAV data collection and manual digitization to assess large wood locations and size allowed relatively large areas to be sampled in an economical manner. Resolution problems were caused by canopy cover, oblique deposition, and shading problems resulting in detection errors. However, under-detection errors were addressed through calibration relationships with field data and the use of standing tree density as an independent variable to correct LW load values from UAV imagery analysis.

The magnitude of the 2017 flood was affected by two anthropogenic factors. First, the intense rainfall has been linked to recent trends of more extreme weather related to global warming effects over the past 30–50 yr. Second, a strong relationship was found between peak flood stage at a particular sampling reach and the percent of non-forest land use in its drainage area. Non-forest land use in the area mainly included pasture and grazing agriculture with some rural suburban and urban developments. This finding underscores the relationship between the combined influence of climate change and land use disturbance to increase flood frequency and magnitude in humanized watersheds that contain ample forested areas, but that may have had a long history of low intensity soil and vegetation disturbance such as in the study area.

Mean stream power can potentially be a good predictor of riparian forest damage by floods since it was positively related to canopy loss during the flood and the percentage of aligned wood pieces that may indicate the frequency of tree toppling. Canopy loss caused by flood damage was highly correlated with cross-sectional and mean stream power and, to a lesser degree, flood depth and relatively narrow valleys. Tabor Creek sustained 61 % canopy loss possibly from it having the highest channel slope and sinuosity of all the study reaches. Canopy losses for the other study reaches were much lower at 11–27 %. Percent aligned LW increased with peak flood discharge and depth, scaled flood depth, and cross-sectional and mean stream power, but not confinement ratio, suggesting that flood power was the main variable influencing LW flow-alignment, as well as tree damage indicated by canopy loss.

Channel and floodplain LW loads showed different relationships with drainage area. Channel loads showed no trend with drainage area. Except for Tabor Creek with loads up to 34 m³/ha, channel loads at the other reaches fluctuated downstream between 13 and 19 m³/ha. Large wood loads in the channel were positively related to narrow valleys and scaled flood depth suggesting that deeper floods can recruit more wood for toppling or channel deposition if wider valley floors are not available for wood storage or flood attenuation. In contrast, LW loads increased dramatically downstream from 6 to 55 m³/ha on floodplains, 16 to 57 m³/ha on terraces, and 7 to 61 m³/ha in chutes. Floodplain deposition is probably controlled by systematic trends in decreasing channel slope and availability of valley floor areas for LW deposition such as the depth and duration of flood inundation, degree of channel widening, frequency of toppling or uprooting of trees, and availability of chutes to direct flow and transport floating wood to distal areas across the valley floor.

Jam density generally increased in reaches with higher standing tree density, lower average bank height, and lower sinuosity channels. The percentage of total wood pieces within a reach deposited in jams decreased with drainage area, scaled HWM depth, and mean stream power. In general, from 50 to 100 % of jams were deposited within a 10

m distance of the channel banks suggesting that higher velocity currents recruited jam wood from the channel margin or as float wood being transported down the channel. Nevertheless, in relatively unconfined reaches 50–75 % of the jams were located on in terraces indicating that floods can move significant LW loads into storage to form jams on higher elevation features across the valley floor in Ozark Highland streams.

This study presents data that can help better understand ecological disturbances in riparian forests caused by extreme floods and be used to support land management practices in Mark Twain National Forest in southern Missouri. Future work will focus on the continued monitoring of these sites to determine the fate of LW stored by the flood of 2017. Channel morphology exerted a significant effect on LW recruitment and deposition during the flood. Single-channel reaches stored >3 times more wood pieces on floodplains and terraces compared to channel areas. In contrast, multithreaded reaches deposited >2 times more wood pieces in channel areas compared to floodplains. Further, jam density generally increased in multithreaded reaches compared to single-channel reaches. Martin et al. (2021) found that channel loads in these North Fork watersheds were like those measured in other rivers in the Ozarks not affected by recent large floods. The present study indicated that channel loads were variable downstream at low to moderate levels. However, LW loads increased dramatically downstream on floodplains, terraces, and in chutes. Thus, floodplains may be buffering LW loads from floods by providing important storages for LW recruited from upstream reaches or nearby channel margins in the Ozark Highlands.

Declaration of competing interest

The authors declare that they have no known competing financial interests or personal relationships that could have appeared to influence the work reported in this paper.

Data availability

Data will be made available on request.

Acknowledgements

This study was supported by award number 1748816 from the National Science Foundation entitled: RAPID: Impacts of an Extreme Flood on River Channel Formation and Riparian Forests. We would like to thank the following people for help during field work: Shay Hostens, Triston Rice, Dylan King, Leah Bournival, Grace Roman, Katy Reminga, Hannah Adams, Sarah LeTarte, Kelly Rose, and Miranda Jordan.

References

- Acker, S.A., Gregory, S.V., Lienkaemper, G., McKee, W.A., Swanson, F.J., Miller, S.D., 2003. Composition, complexity, and tree mortality in riparian forests in the central Western Cascades of Oregon. *For. Ecol. Manag.* 173, 293–308.
- Adamski, J.C., Petersen, J.C., Freiwald, D.A., Davis, J.V., 1995. Environmental and hydrologic setting of the Ozark Plateaus study unit, Arkansas, Kansas, Missouri, and Oklahoma. In: USGS Water-Resources Investigations Report, pp. 94–4022.
- Alexander, T.W., Wilson, G.L., 1995. Technique for estimating the 2- to 500-year flood discharges on unregulated streams in rural Missouri. In: Water-Resources Investigations Report, 95, pp. 1–33.
- Alfieri, L., Bissellink, B., Dottori, F., Naumann, G., de Roo, A., Salamon, P., Wyser, K., Feyen, L., 2017. Global projections of river flood risk in a warmer world. *Earth's Future* 5, 171–182.
- Allen, M.S., Thapa, V., Arévalo, J.R., Palmer, M.W., 2012. Windstorm damage and forest recovery: accelerated succession, stand structure, and spatial pattern over 25 years in two Minnesota forests. *Plant Ecol.* 213, 1833–1842.
- Anderson, K., Gaston, K.J., 2013. Lightweight unmanned aerial vehicles will revolutionize spatial ecology. *Front. Ecol. Environ.* 11, 138–146.
- Andréasson, J., Bergström, S., Carlsson, B., Lindström, G., Graham, L.P., 2004. Hydrological Change: climate Change Impact Simulations for Sweden. *Swed. Region. Clim.Modell. Prog.* 33, 228–234.
- Atha, J.B., Dietrich, J.T., 2016. Detecting fluvial wood in forested watersheds using LiDAR data: a methodological assessment. *River Res. Appl.* 32, 1587–1596.

- Bendix, J., 1994. Scale, direction, and pattern in riparian vegetation-environment relationships. *Ann. Assoc. Am. Geogr.* 84, 652–665.
- Bendix, J., 1997. Flood disturbance and the distribution of riparian species diversity. *Geogr. Rev.* 87, 468.
- Bendix, J., 1999. Stream power influence on southern Californian riparian vegetation. *J. Veg. Sci.* 10, 243–252.
- Bendix, J., Hupp, C.R., 2000. Hydrological and geomorphological impacts on riparian plant communities. *Hydrol. Process.* 14, 2977–2990.
- Blauch, G.A., Jefferson, A.J., 2019. If a tree falls in an urban stream, does it stick around? Mobility, characteristics, and geomorphic influence of large wood in urban streams in northeastern Ohio, USA. *Geomorphology* 337 (15), 1–14.
- Booth, D.B., Hartley, D., Jackson, R., 2002. Forest cover, impervious-surface area, and the mitigation of stormwater impacts. *J. Am. Water Resour. Assoc.* 38 (3), 835–845.
- Bren, L.J., 1993. Riparian zone, stream, and floodplain issues: a review. *J. Hydrol.* 150 (2–4), 277–299.
- Brewer, C.W., Linnartz, N.E., 1973. The recovery of hurricane-bent loblolly pine. In: Louisiana State University Forestry Note 104. Louisiana State University, Baton Rouge.
- Brierley, G.J., Fryirs, K.A., 2005. *Geomorphology and River Management: Applications of the River Styles Framework*. Blackwell Publishing, Malden, Massachusetts.
- Brookshire, B.L., Jensen, R., Dey, D.C., 1997. The Missouri Ozark Forest Ecosystem Project: past, present, and future. In: Brookshire, B.L., Shifley, S.R. (Eds.), *Proceedings of the Missouri Ozark Forest Ecosystem Project Symposium: An Experimental Approach to Landscape Research*, June 3–5; St. Louis, MO. General Technical Report NC-193. U.S. Department of Agriculture, Forest Service, North Central Forest Experiment Station, St. Paul, MN, pp. 1–25.
- Bull, W.B., 1979. Threshold of critical power in streams: discussion and reply. *Geol. Soc. Am. Bull.* 90, 453–464.
- Bunte, K., Abt, S.R., 2001. Sampling surface and subsurface particle-size distributions in wadable gravel- and cobble-bed stream for analyses in sediment transport, hydraulics, and streambed monitoring. In: General Technical Report RMRS-GTR-74. U.S. Department of Agriculture, Forest Service, Rocky Mountain Research Station, Fort Collins, CO.
- Busing, R.T., Fujimori, T., 2005. Biomass, production and woody detritus in an old coast redwood (*Sequoia sempervirens*) forest. *Plant Ecol.* 177 (2), 177–188.
- Carling, P., Jansen, J., Meshkova, L., 2014. Multichannel rivers: their definition and classification. *Earth Surf. Process. Landf.* 39, 26–37.
- Chang, H., Knight, C.G., Staneva, M.P., Kostov, D., 2002. Water resource impacts of climate change in southwestern Bulgaria. *GeoJournal* 57, 159–168.
- Chao, K.-J., Phillips, O.L., Baker, T.R., 2008. Wood density and stocks of coarse woody debris in a northwestern Amazonian landscape. *Can. J. For. Res.* 38 (4), 795–805.
- Chow, V.T., 1959. *Open-Channel Hydraulics*. Blackburn Press, Caldwell, NJ.
- Christensen, D.L., Herwig, B.R., Schindler, D.E., Carpenter, S.R., 1996. Impacts of lakeshore residential development on coarse woody debris in north temperate lakes. *Ecol. Appl.* 6 (4), 1143–1149.
- Collins, B.D., Montgomery, D.R., Fetherston, K.L., Abbe, T.B., 2012. The floodplain large-wood cycle hypothesis: a mechanism for the physical and biotic structuring of temperate forested alluvial valleys in the North Pacific coastal ecoregion. *Geomorphology* 139–140, 460–470.
- Comiti, F., Lucia, A., Rickenmann, D., 2016. Large wood recruitment and transport during large floods: a review. *Geomorphology* 269, 23–39.
- Cordova, J.M., Rosi-Marshall, E.J., Yamamoto, A.M., Lamberti, G.A., 2007. Quantify, controls and functions of large woody debris in Midwestern USA streams. *River Res. Appl.* 23, 21–33.
- Costa, J.E., O'Connor, J.E., 1995. Geomorphically effective floods. In: *Geophysical Monograph* 89, Natural and Anthropogenic Influences in Fluvial Geomorphology, pp. 45–56.
- Dandois, J.P., Ellis, E.C., 2010. Remote sensing of vegetation structure using computer vision. *Remote Sens.* 2, 1157–1176.
- Dandois, J., Olano, M., Ellis, E., 2015. Optimal altitude, overlap, and weather conditions for computer vision UAV estimates of forest structure. *Remote Sens.* 7, 13895–13920.
- Daniels, R.B., Gilliam, J.W., 1996. Sediment and chemical load reduction by grass and riparian filters. *Soil Sci. Soc. Am. J.* 60, 246–251.
- Duley, J.W., Boswell, C., Prewett, J., 2015. Recharge Area of Selected Large Springs in the Ozarks. Sinkholes and the Engineering and Environmental Impacts of Karst: Proceedings of the Fourteenth Multidisciplinary Conference.
- Dwire, K.A., Mellmann-Brown, S., Gurrieri, J.T., 2018. Potential effects of climate change on riparian area, wetland, and groundwater-dependent ecosystems in the Blue Mountains, Oregon, USA. *Clim. Serv.* 10, 44–52.
- Eisenhies, H.H., Aust, W.M., Burger, J.A., Adams, M.B., 2007. Forest operations, extreme flooding events, and considerations for hydrologic modeling in the Appalachians. *For. Ecol. Manag.* 242, 77–98.
- Engelhardt, B.M., Weisberg, P.J., Chambers, J.C., 2011. Influences of watershed geomorphology on extent and composition of riparian vegetation. *J. Veg. Sci.* 23, 127–139.
- Erdman, J., 2017. Record Flooding in April/May 2017 Swamps Parts of Missouri, Arkansas. The Weather Channel, Illinois.
- Everham, E.M., Brokaw, N.V.L., 1996. Forest damage and recovery from catastrophic wind. *Bot. Rev.* 62, 113–185.
- Fierke, M.K., Kauffman, J.B., 2006. Riverscape-level patterns of riparian plant diversity along a successional gradient, Willamette river, Oregon. *Plant Ecol.* 185, 85–95.
- Finn, A., Kumar, P., Peters, S., O'Hehir, J., 2022. Unsupervised spectral-spatial processing of drone imagery for identification of pine seedlings. *J. Photogramm. Remote Sens.* 183, 363–388.
- Fischer, S., Greet, J., Walsh, C.J., Catford, J.A., 2021. Flood disturbance affects morphology and reproduction of woody riparian plants. *Sci. Rep.* 11, 16477.
- Flanagan, P., Mahmood, R., 2021. Spatiotemporal analysis of extreme precipitation in the Missouri River Basin from 1950 to 2019. *J. Appl. Meteorol. Climatol.* 60, 811–827.
- Fonstad, M.A., Dietrich, J.T., Courville, B.C., Jensen, J.L., Carbonneau, P.E., 2013. Topographic structure from motion: a new development in photogrammetric measurement. *Earth Surf. Process. Landf.* 38, 421–430.
- Friedman, J.M., Lee, V.J., 2002. Extreme floods, channel change, and riparian forests along ephemeral streams. *Ecol. Monogr.* 72, 409–425.
- Fujita, T., Itaya, A., Miura, M., Manabe, T., Yamamoto, S., 2003. Canopy structure in a temperate old-growth evergreen forest analyzed by using aerial photographs. *Plant Ecol.* 168, 23–29.
- Fuller, I.C., 2007. Geomorphic work during a “150-year” storm: contrasting behaviors of river channels in a New Zealand catchment. *Ann. Assoc. Am. Geogr.* 97, 665–676.
- Garssen, A.G., Baattrup-Pedersen, A., Voeselek, L.A.C.J., Verhoeven, J.T.A., Soons, M.B., 2015. Riparian plant community responses to increased flooding: a meta-analysis. *Glob. Chang. Biol.* 21, 2881–2890.
- Garssen, A.G., Baattrup-Pedersen, A., Riis, T., Raven, B.M., Hoffman, C.C., Verhoeven, J.T.A., Soons, M.B., 2017. Effects of increased flooding on riparian vegetation: field experiments simulating climate change along five European lowland streams. *Glob. Chang. Biol.* 23, 1–12.
- Gerke, D., 2019. An Evaluation of Unmanned Aerial Systems and Structure-from-motion for Fluvial Large Wood Sensing and Risk Assessment. Master's thesis 5100., Department of Geography, Western Michigan University.
- Getzin, S., Wiegand, K., Schöning, I., 2012. Assessing biodiversity in forests using very high-resolution images and unmanned aerial vehicles. *Methods Ecol. Evol.* 3, 397–404.
- Guerra-Hernández, J., Díaz-Varela, R.A., Álvarez-González, J.G., 2021. Assessing a novel modelling approach with high resolution UAV imagery for monitoring health status in priority riparian forests. *For. Ecosystems* 8, 61. <https://doi.org/10.1186/s40663-021-00342-8>.
- Guiney, M.R., Lininger, K.B., 2021. Disturbance and valley confinement: controls on floodplain large wood and organic matter jam deposition in the Colorado Front Range, USA. *Earth Surf. Process. Landf.* 2022, 1–19.
- Guldin, J.M., 2008. A history of forest management in the Ozark Mountains. In: Guldin, J.M., Iffrig, G.F., Flader, S.L. (Eds.), *Pioneer Forest: A half-century of sustainable uneven-aged forest management in the Missouri Ozarks*. Gen. Tech. Rep. SRS-108. U.S. Department of Agriculture, Forest Service, Southern Research Station, Asheville, NC, pp. 3–8.
- Gurnell, A.M., Piegay, H., Swanson, F.J., Gregory, S.V., 2002. Large wood and fluvial processes. *Freshw. Biol.* 47, 601–619.
- Hanberry, B.B., Jones-Farrand, D.T., Kabrick, J.M., 2014. Historical open forest ecosystems in the Missouri Ozarks: reconstruction and restoration targets. *Ecol. Restor.* 32 (4), 07–416.
- Harrelson, C.C., Rawlins, C.L., Potyondy, J.P., 1994. Stream channel reference sites: an illustrated guide to field technique. In: United States Department of Agriculture, Forest Service, Rocky Mountain Research Station, General Technical Report RM-245.
- Harrison, L.R., Dunne, T., Fisher, G.B., 2015. Hydraulic and geomorphic processes in an overbank flood along a meandering, gravel-bed river: implications for chute formation. *Earth Surf. Process. Landf.* 40, 1239–1253.
- Hauer, R.R., Smith, R.D., 1998. The hydrogeomorphic approach to functional assessment of riparian wetlands: evaluating impacts and mitigation Ono river floodplains of the U.S.A. *Freshw. Biol.* 40, 517–530.
- Heimann, D.C., Holmes, R.R., Harris, T.E., 2018. Flooding in the Southern Midwestern United States, April–May 2017. Open-File Report.
- Herring, D., Gerhard, M., Manderbach, R., Reich, M., 2004. Impact of a 100-year flood on vegetation, benthic invertebrates, riparian fauna, and large woody debris standing stock in an alpine floodplain. *River Res. Appl.* 20, 445–457.
- Hostens, D.S., Dogwiler, T., Hess, J.W., Pavlowsky, R.T., Bendix, J., Martin, D.T., 2022. Assessing the role of sUAS mission design in the accuracy of digital surface models derived from structure-from-motion photogrammetry. In: Konsoer, K., Leitner, M., Lewis, Q. (Eds.), *sUAS Applications in Geography, Springer Nature, Geotechnologies and the Environment Series*, 24. <https://link.springer.com/book/10.1007/978-3-03-1-01976-0>.
- Hu, Q., Willson, G.D., Chen, X., Akyuz, A., 2005. Effects of climate and landcover change on stream discharge in the Ozark Highlands, USA. *Environ. Model. Assess.* 10, 9–19.
- Hupp, C.R., Bornette, G., 2005. Vegetation as a tool in the interpretation of fluvial geomorphic processes and landforms in humid temperate areas. In: *Tools in Fluvial Geomorphology*, pp. 269–288.
- Hupp, C.R., Osterkamp, W.R., 1996. Riparian vegetation and fluvial geomorphic processes. *Geomorphology* 14, 277–295.
- Huylenbroeck, L., Latte, N., Lejeune, P., Georges, B., Claessens, H., Michez, A., 2021. What factors shape spatial distribution of biomass in riparian forests? Insights from a LiDAR survey over a large area. *Forests* 12, 371.
- Jacobson, R.B., Gran, K.B., 1999. Gravel sediment routing from widespread, low-intensity landscape disturbance, Current River Basin, Missouri. *Earth Surf. Process. Landf.* 24, 897–917.
- Jaramillo, V.J., Kaufman, J.B., Renteria-Rodriguez, L., Cummings, D.L., Ellingson, L.J., 2003. Biomass, carbon, and nitrogen pools in Mexican tropical dry forest landscapes. *Ecosystems* 6 (7), 609–629.
- Jeong, E., Park, J.-Y., Hwang, C.-S., 2018. Assessment of UAV photogrammetric mapping accuracy in the beach environment. *J. Coast. Res.* 85, 176–180.
- Johnson, S.L., Swanson, F.J., Grant, G.E., Wondzell, S.M., 2000. Riparian forest disturbances by a mountain flood — the influence of floated wood. *Hydrol. Process.* 14, 3031–3050.

- Katz, G.L., Friedman, J.M., Beatty, S.W., 2005. Delayed effects of flood control on a flood-dependent riparian forest. *Ecol. Appl.* 15, 1019–1035.
- Kaufmann, P.R., Levine, P., Robison, E.G., Seeliger, C., Peck, D.V., 1999. Quantifying physical habitat in Wadeable streams. In: EPA-620-R-99-003. U.S. Environmental Protection Agency, Washington, D.C.
- Keller, E.A., Swanson, F.J., 1979. Effects of large organic material on channel form and fluvial processes. *Earth Surf. Process.* 4, 361–380.
- Keys, T.A., Governor, H., Jones, C.N., Hession, W.C., Hester, E.T., Scott, D.T., 2018. Effects of large wood on floodplain connectivity in a headwater Mid-Atlantic stream. *Ecol. Eng.* 118, 134–142.
- Kondolf, G.M., Piegay, H., Landon, N., 2007. Changes in the riparian zone of the lower Eygues River, France, since 1830. *Landscape Ecol.* 22, 367–384.
- Kraft, C.E., Schneider, R.L., Warren, D.R., 2002. Ice storm impacts on woody debris and debris dam formation in northeastern U.S. streams. *Can. J. Fish. Aquat. Sci.* 59, 1677–1684.
- Kramer, K., Wohl, E., 2017. Rules of the road: a qualitative and quantitative synthesis of large wood transport through drainage networks. *Geomorphology* 279, 74–97.
- Kramer, K., Vreugdenhil, S.J., van der Werf, D.C., 2008. Effects of flooding on the recruitment, damage, and mortality of riparian tree species: a field and simulation study on the Rhine floodplain. *For. Ecol. Manag.* 255, 3893–3903.
- Kupfer, J.A., Myers, A.T., Mclane, S.E., Melton, G.N., 2008. Patterns of forest damage in a southern Mississippi landscape caused by hurricane Katrina. *Ecosystems* 11, 45–60.
- Lapides, A.A., Manga, M., 2020. Large wood as a confounding factor in interpreting the width of spring-fed streams. *Earth Surf. Dyn.* 8, 195–210.
- Latterell, J.J., Naiman, R.J., 2007. Sources and dynamics of large logs in a temperate floodplain river. *Ecol. Appl.* 17 (4), 1127–1141.
- Lecce, S.A., 1997. Nonlinear downstream changes in stream power on Wisconsin Blue River. *Ann. Assoc. Am. Geogr.* 87, 471–486.
- Leopold, L.B., Wolman, M.G., 1957. River Channel Patterns: Braided, Meandering, and Straight. US Geological Survey Professional Paper 282-B.
- Lininger, K.B., Wohl, E., Sutfin, N.A., Rose, J.R., 2017. Floodplain downed wood volumes: a comparison across three biomes. *Earth Surf. Process. Landf.* 42, 1248–1261.
- Lininger, K.B., Scamardo, J.E., Guiney, M.R., 2021. Floodplain large wood and organic matter jam formation after a large flood: investigating the influence of floodplain forest stand characteristics and river corridor morphology. *Journal of Geophysical Research-Earth Surface* 126 (6), e2020JF006011.
- Lopez, R.D., Nash, M.S., Heggem, D.T., Ebert, D.W., 2008. Watershed vulnerability predictions for the Ozarks using landscape models. *J. Environ. Qual.* 37, 1769–1780.
- Lowrance, R., 1998. Riparian forest ecosystems as filters for nonpoint-source pollution. In: Pace, M.L., Groffman, P.M. (Eds.), *Success, Limitations, and Frontiers in Ecosystems Science*, pp. 113–141.
- Guyette, R.P., Dey, D.C., Stambaugh, M.C., 2008. The temporal distribution and carbon storage of large oak wood in streams and floodplain deposits. *Ecosystems* 11, 643–653.
- Lyon and Sagers, n.d. Lyon, J., and C.L. Sagers (n.d.). Structure of herbaceous plant assemblages in a forested riparian landscape. *Plant Ecology* 138, 1–16.
- Marcus, W.A., Marston, R.A., Colvard Jr., C.R., Gray, R.D., 2002. Mapping the spatial and temporal distributions of woody debris in stream in the Greater Yellowstone Ecosystem, USA. *Geomorphology* 44, 323–335.
- Martin, D.J., Pavlowsky, R.T., 2011. Spatial patterns of channel instability along an Ozark River, Southwest Missouri. *Phys. Geogr.* 32, 445–468.
- Martin, D.J., Harden, C.P., Tran, L., Pavlowsky, R.T., 2018. Investigating patterns of in-channel wood deposition locations in a low-gradient, variable-confined alluvial river system. *Prog. Phys. Geogr.* 42, 139–161.
- Martin, D.J., Pavlowsky, R.T., Bendix, J., Dogwiler, T., Hess, J., 2021. Impacts of an extreme flood on large wood recruitment and transport processes. *Phys. Geogr.* <https://doi.org/10.1080/02723646.2021.1980958>.
- Martinez-Fernandez, V., Van Oorschot, M., De Smitte, J., Gonzalez del Tanago, M., Buijse, A.D., 2018. Modelling feedbacks between geomorphological and riparian vegetation responses under climate change in a Mediterranean context. *Earth Surf. Process. Landf.* 43, 1825–1835.
- Meitzen, K.M., Phillips, J.N., Perkins, T., Manning, A., Julian, J.P., 2018. Catastrophic flood disturbance and a community's response to plant resilience in the heart of the Texas Hill Country. *Geomorphology* 305, 20–32.
- Meyer, W.B., 1995. Past and Present Land Use and Land Cover in the U.S.A.: Consequences: The Nature and Implications of Environmental Change [Consequences: Nat. Implications Environ. Change], 1 no. 1.
- Midwestern Regional Climate Center (MRCC), 2019. Cli-MATE. Website. Midwestern Regional Climate Center. <https://mrcc.illinois.edu/CLIMATE/Station/Annual/StnAnnualBTD2.jsp>.
- Miller, A.J., 1990. Flood hydrology and geomorphic effectiveness in the central Appalachians. *Earth Surf. Process. Landf.* 15, 119–134.
- Miller, S.M., Wilkerson, T.F., 2001. North Fork River Watershed Inventory and Assessment, Missouri Department of Conservation.
- Missouri Spatial Data Information Service (MSDIS), 2011. Digital Elevation Model Data. <https://www.msdis.missouri.edu/data/Elevation/index.html>.
- Mohan, M., Silva, C.A., Klauber, C., Jat, P., Catts, G., Cardil, A., Hudak, A.T., Dia, M., 2017. Individual tree detection from unmanned aerial vehicle (UAV) derived canopy height model in an open canopy mixed conifer forest. *Forests* 8, 340.
- Montgomery, D.R., Abbe, T.B., 2006. Influence of logjam-formed hard points on the formation of valley-bottom landforms in an old-growth forest valley, Queets River, Washington, USA. *Quat. Res.* 65, 147–155.
- Montgomery, D.R., MacDonald, L.H., 2002. Diagnostic approach to stream channel assessment and monitoring. *J. Am. Water Resour. Assoc.* 38, 1–16.
- Montgomery, D.R., Buffington, J.M., Smith, R.D., Schmidt, K.M., Pess, G., 1995. Pool spacing in forest channels. *Water Resources Research* 31 (4), 1097–1105.
- Montgomery, D.R., Abbe, T.B., Buffington, J.M., Peterson, N.P., Schmidt, K.M., Stock, J. D., 1996. Distribution of bedrock and alluvial channels in forested mountain drainage basins. *Nature* 381, 587–589.
- Montgomery, D.R., Collins, B.D., Buffington, J.M., Abbe, T.B., 2003. Geomorphic effects of wood in rivers. In: Gregory, S.V., Boyer, K.L., Gurnell, A.M. (Eds.), *The Ecology and Management of Wood in World Rivers*, Symposium, 37. American Fisheries Society, Bethesda, Maryland.
- Morche, David, et al., 2007. Hydrology and geomorphic effects of a high-magnitude flood in an alpine river. *Geogr. Ann. Ser. B* 89 (1), 5–19.
- Moulin, B., Schenck, E.R., Hupp, C.R., 2011. Distribution and characterization of in-channel large wood in relation to geomorphic patterns on a low-gradient river. *Earth Surf. Process. Landf.* 36, 1137–1151.
- Multi-Resolution Land Characteristics (MRLC) Consortium, 2016. National Land Cover Database (NLCD) 2016 Land Cover (CONUS). <https://www.mrlc.gov/data/?f%5B0%5D=region%3Aconus>.
- Murphy, M.L., Koski, K.V., 1989. Input and Depletion of Woody Debris in Alaska Streams and Implications for Streamside Management. *N. Am. J. Fish. Manag.* 9, 427–436.
- Nagel, D.E., Buffington, J.M., Parkes, S.L., Wenger, S., Goode, J.R., 2014. A Landscape Scale Valley Confinement Algorithm: Delineating Unconfined Valley Bottoms for Geomorphic, Aquatic, and Riparian Applications.
- Naiman, R.J., Decamps, H., 1997. The ecology of interfaces: riparian zones. *Annu. Rev. Ecol. Syst.* 28, 621–658.
- Naiman, R.J., Decamps, H., McClain, M.E., 2005. RIPARIA: Ecology, Conservation, and Management of Streamside Communities. Elsevier Academic Press, Amsterdam.
- Nakamura, F., Swanson, F.J., 1994. Distribution of coarse woody debris in a mountain stream, western Cascade Range, Oregon. *Can. J. For. Res.* 24, 2395–2403.
- Nanavati, W.P., Grimm, E.C., 2020. Humans, fire, and ecology in the southern Missouri Ozarks, USA. *The Holocene* 30 (1), 125–135.
- Nearby, D.G., Buschmann, S., Ffolliott, P.F., 2010. Function of riparian vegetation in retaining sediment in watersheds. In: *Hydrology and Water Resources in Arizona and the Southwest*, 40, pp. 31–44.
- Nigh, T.A., Schroeder, W.A., 2002. Atlas of Missouri Ecoregions. Missouri Department of Conservation. The Conservation Commission—State of Missouri.
- O'Connor, J.E., Costa, J.E., 2004. Spatial distribution of the largest rainfall-runoff floods from basin between 2.6 and 26,000 km² in the United States and Puerto Rico. *Water Resour. Res.* 40, W01107.
- Olson, D.H., Anderson, P.D., Frissell, C.A., Welsh Jr., H.H., Bradford, D.F., 2007. Biodiversity management approaches for stream-riparian areas: perspectives for Pacific Northwest headwater forests, microclimates, and amphibians, 2007. *For. Ecol. Manag.* 246, 81–107.
- Owen, M.R., Pavlowsky, R.T., Womble, P.J., 2011. Historical disturbance and contemporary floodplain development along an Ozark river, southwest Missouri. *Phys. Geogr.* 32 (5), 423–444.
- Palik, B., Golladay, W., Goebel, P.C., Taylor, B.W., 1998. Geomorphic variation in riparian tree mortality and stream coarse woody debris recruitment from record flooding in a coastal plain stream. *Ecoscience* 5 (4), 551–560.
- Panfil, M.S., Jacobson, R.B., 2001. Relations among geology, physiography, land use, and stream habitat conditions in the Buffalo and Current River systems, Missouri and Arkansas. In: United States Geological Survey, Biological Resources Division, Biological Science Report USGS/BRD/BSR-2001-0005.
- Pavlowsky, R.T., Owen, M.R., Bradley, R.A., 2016. Recent increase in extreme rainfall amounts in the Big Barren Creek Watershed, S.E. Missouri. *Missouri Natural Areas Newsletter* 16, 19–24.
- Perry, L.G., Anderson, D.C., Reynolds, L.V., Nelson, S.M., Shafroth, P.B., 2012. Vulnerability of riparian ecosystems to elevated CO₂ and climate change in arid and semiarid western North America. *Glob. Chang. Biol.* 18, 821–842.
- Piegay, H., Marston, R.A., 1998. Distribution of large woody debris along the outer bend of meanders in the Ain River, France. *Phys. Geogr.* 19, 318–340.
- Poff, N.L., 2002. Ecological response to and management of increased flooding causes by climate change. *Philos. Trans. R. Soc. Lond.* 360, 1497–1510.
- Poff, N.L., Tokar, S., Johnson, P., 1996. Stream hydrological and ecological responses to climate change assessed with an artificial neural network. *Limnol. Oceanogr.* 41, 857–863.
- Polednikova, Z., Galia, T., 2021. Ecosystem services of large wood: mapping the research gap. *Water* 13, 2594.
- Pollock, M.M., Beachie, T.J., Wheaton, J.M., Jordan, C.E., Bouwes, N., Weber, N., Volk, C., 2014. Using beaver dams to restore incised stream ecosystems. *Bioscience* XX, 1–12.
- Polvi, L.E., Wohl, E., 2013. Biotic drivers of stream planform: implications for understanding the past and restoring the future. *BioScience* 63 (6), 439–452.
- Quilter, M., Anderson, V., 2000. Low altitude/large scale aerial photographs: a tool for range and resource managers. *Rangelands* 22, 13–17.
- Raeker, G.W., Moser, K., Butler, B.J., Fleming, J., Gormanson, D.D., Hansen, M.H., Kurtz, C.M., Miles, P.D., Morris, M., Treiman, T.B., 2010. Missouri's Forests 2008. Resource Bulletin. NRS-54.
- Ray, J.H., 2009. Geoaerchaeological investigations in the Upper North Fork River Valley in southern Missouri. *Plains Anthropol.* 54 (210), 137–154.
- Rosgen, D.R., 1996. Applied River Morphology. Wildland Hydrology, Pagosa Springs, Colorado.
- Ruiz-Villanueva, H., Piegay, A.M., Gurnell, R.A., Marston, M.Stoffel, 2016. Recent advances quantifying the large wood dynamics in river basins: new methods and remaining challenges. *Rev. Geophys.* 54, 611–652.

- Ruiz-Villanueva, V., Wyzga, B., Hajdukiewicz, H., Stoffel, M., 2016. Exploring large wood retention and deposition in contrasting river morphologies linking numerical modeling and field observations. *Earth Surf. Process. Landf.* 41, 446–459.
- Ruiz-Villanueva, V.B., Badoux, A., Rickerenmann, D., Bockli, M., Schafli, S., Steeb, N., Stoffel, M., Rickli, C., 2018. Impacts of a large flood along a mountain river basin: the importance of channel widening and estimating the large wood budget in the upper Emme River (Switzerland). *Earth Surface Dynamics* 6, 1115–1137.
- Ruiz-Villanueva, V., Mazzaorana, B., Blade, E., Burkli, L., Iribarren-Anacona, P., Mao, L., Nakamura, F., Ravazzolo, D., Rickermann, D., Sanz-ramos, M., Stoffel, M., Wohl, E., 2019. Characterization of wood-laden flows in rivers. *Earth Surf. Process. Landf.* 44, 1694–1709.
- Saint-Laurent, D., Arsenault-Boucher, L., Berthelot, J.-S., 2019. Contrasting effects of flood disturbances on alluvial soils and riparian tree structure and species composition in mixed temperate forests. *Air Soil Water Res.* 12, 1–15.
- Sanhueza, D., Picco, L., Ruiz-Villanueva, V., Iroume, A., Ulloa, H., Barrientos, G., 2019. Quantification of fluvial wood using UAVs and structure from motion. *Geomorphology* 345, 106837.
- Sauer, C.O., 1920. *The Geography of the Ozark Highland of Missouri*. The University of Chicago Press, Chicago, IL.
- Scott, D.N., Wohl, E.E., 2018. Natural and anthropogenic controls on wood loads in river corridors of the Rocky, Cascade, and Olympic Mountains. *USA. Water Resour. Res.* 54, 7893–7909.
- Seavy, N.E., Gardali, T., Golet, G.H., Griggs, F.T., Howell, C.A., Kelsey, R., Small, S.L., Viers, J.H., Weigand, J.F., 2009. Why climate change makes riparian restoration more important than ever. *Ecol. Restor.* 27, 330–338.
- Slater, L.J., Villarini, G., 2016. Recent trends in U.S. flood risk. *Geophys. Res. Lett.* 43 <https://doi.org/10.1002/2016GL071199>.
- Solari, L., Van Oorshot, M., Belletti, B., Hendriks, D., Rinaldi, M., Vargas-Luna, A., 2016. Advances on modelling riparian vegetation-hydromorphology interactions. *River Res. Appl.* 32, 164–178.
- Stambaugh, M.C., Muzika, R.M., Guyette, R.P., 2002. Disturbance characteristics and overstory composition of an old-growth shortleaf pine (*Pinus echinata* Mill.) forest in the Ozark Highlands, Missouri, USA. *Nat. Areas J.* 22, 108–119.
- Steele, K.L., Kabrick, J.M., Dey, D.C., Jensen, R.G., 2013. Restoring riparian forests in the Missouri Ozarks. *North. J. Appl. For.* 30, 109–117.
- Steiger, J., Tabachi, E., Dufour, S., Corenblit, D., Peiry, J.-L., 2005. Hydrogeomorphic processes affecting riparian habitat withing alluvial channel-floodplain river systems: a review for the temperate zone. *River Res. Appl.* 21, 719–737.
- Stephens, S.L., Fry, D.L., Franco-Vizcaíno, E., 2008. Wildfire and Spatial patterns in Forests in Northwestern Mexico: the United States wishes it had similar fire problems. *Ecol. Soc.* 13.
- Stout, J.C., Rutherford, I.D., Gorge, J., Webb, A.J., Kitchingman, A., Tonkin, Z., Lyon, J., 2018. Passive recovery of wood loads in rivers. *Water Resources Research* 54, 8828–8846.
- Stufin, N.A., Wohl, E.E., Dwire, K.A., 2016. Banking carbon: a review of organic carbon storage and physical factors influencing retention in floodplains and riparian ecosystems. *Earth Surf. Process. Landf.* 41, 38–60.
- Swanson, F.J., Johnson, S.L., Gregory, S.V., Acker, S.A., 1998. Flood disturbance in a forested mountain landscape. *Bioscience* 48, 681–689.
- Tal, M., Gran, K., Murray, A.B., Paola, C., Hicks, D.M., 2004. Riparian vegetation as a primary control on channel characteristics in multi-thread rivers. In: *Riparian Vegetation and Fluvial Geomorphology Water Science and Application*, pp. 43–58.
- Thornberry-Ehrlich, T.L., 2016. *Ozark National Scenic Riverways, Geologic Resources Inventory Report, Natural Resources Report NPS/NRSS/GRD/NRR-2016/1307*. U.S. Department of Interior, National Park Service, Fort Collins, Colorado. <http://npsistory.com/publications/ozar/nrr-2016-1307.pdf>.
- Turner, M.G., Carpenter, S.R., Gustafson, E.J., Naiman, R.J., Pearson, S.M., 1998. Land use. In: Mac, M.J., Opler, P.A., Doran, P., Haecker, C. (Eds.), *Status and Trends of our Nation's Biological Resources*, 1. National Biological Service, Washington, DC.
- United States Department of Agriculture (USDA), 2005. *Soil Survey of Douglas County, Missouri*. National Cooperative Soil Survey.
- United States Department of Agriculture (USDA), 2006. *Soil Survey of Howell County, Missouri*. National Cooperative Soil Survey.
- United States Department of Agriculture (USDA) – Farm Production and Conservation Business Center (FPAC-BC) Geospatial Enterprise Operations (GEO) Branch, 2016. *National Agriculture Imagery Program (NAIP)*. <https://naip-usdaonline.hub.arcgis.com/>.
- US Department of Commerce, NOAA, National Weather Service, 2017. *Historic Flooding Event – 28-30 April 2017*. National Weather Service.
- Vanlooy, J.A., Martin, C.W., 2005. Channel and vegetation change on the Cimarron River, Southwestern Kansas, 1953–2001. *Annals of the Association of American Geographers* 95, 727–739.
- Venarsky, M.P., Walters, D.M., Hall Jr., R.O., Livers, B., Wohl, E., 2018. Shifting stream planform state decreases stream productivity yet increases riparian animal production. *Oecologia* 187, 167–180.
- Vigiak, O., Malago, A., Biouraoui, F., Grizzetti, B., Weissteiner, C.J., Pastori, N.M., 2016. Impact of current riparian land on sediment retention in the Danube River Basin. *Sustainability Water Qual. Ecol.* 8, 30–49.
- Vought, L.B.-M., Dahl, J., Pedersen, C.L., Lacoursiere, J.O., 1994. Nutrient retention in riparian ecotones. *Ambio* 23 (6), 342–.
- Ward, D., Trimble, S.W., 2003. *Environmental Hydrology (2nd)*. CRC Press, Taylor Francis Group, Boca Raton.
- Warren, D.R., Kraft, C.E., Keeton, W.S., Nunery, J.S., Likens, G.E., 2009. Dynamics of wood recruitment in streams of the northeastern US. *For. Ecol. Manag.* 258, 804–813.
- Warrick, J.A., Ritchie, A.C., Adelman, G., Adelman, K., Limber, P.W., 2017. New techniques to measure cliff change from historical oblique aerial photographs and structure-from-motion photogrammetry. *J. Coast. Res.* 331, 39–55.
- Watanabe, Y., Kawahara, Y., 2016. UAV Photogrammetry for monitoring changes in river topography and vegetation. *Procedia Eng.* 154, 317–325.
- Welling, R.T., Wilcox, A.C., Dixon, J.L., 2021. Large wood and sediment storage in a mixed bedrock-alluvial stream, western Montana, USA. *Geomorphology* 384, 107703.
- Wing, O.E., Lehman, W., Bates, P.D., Sampson, C.C., Quinn, N., Smith, A.M., Neal, J.C., Porter, J.R., Kousky, C., 2022. Inequitable patterns of US flood risk in the Anthropocene. *Nat. Clim. Chang.* 12, 156–162.
- Wohl, E., 2013. *Floodplains and Wood*. *Earth Sci. Rev.* 123, 194–212.
- Wohl, E., 2017. Bridging gaps: an overview of wood across time and space in diverse rivers. *Geomorphology* 279, 3–26.
- Wohl, E., Iskin, E.P., 2022. The transience of channel-spanning logjams in mountain streams. *Water Resour. Res.* 58, e2021WR031556.
- Wohl, E., Jaeger, K., 2009. A conceptual model for the longitudinal distribution of wood in mountain streams. *Earth Surf. Process. Landf.* 34, 329–344.
- Wohl, E., Scamardo, J., 2022. Patterns of organic matter accumulation in dryland river corridors of the southwestern United States. *Sci. Total Environ.* 833, 155136.
- Wohl, E., Scott, D.N., 2016. Wood and sediment storage and dynamics in river corridors. *Earth Surf. Process. Landf.* 42 (1), 5–23.
- Wohl, E., Cenderelli, D.A., Dwire, K.A., Ryan-Burkett, S.E., Young, M.K., Fausch, K.D., 2010. Large in-stream wood studies: a call for common metrics. *Earth Surface Processes and Landform* 35, 618–625.
- Wohl, E., Scott, D.N., Lininger, K.B., 2018. Spatial distribution of channel and floodplain large wood in forested river corridors of the Northern Rockies. *Water Resour. Res.* 54 (10), 7879–7892.
- Wohl, E., Kramer, N., Ruiz-Villanueva, V., Scott, D.N., Comti, F., Gurnell, A.M., Piegay, H., Lininger, K.B., Jaeger, K.L., Waters, D.M., Fausch, K.D., 2019. The natural wood regime in rivers. *Bioscience* 69 (4), 259–273.
- Wolman, M.G., 1954. A method of sampling coarse river-bed material. *Trans. Am. Geophys. Union* 35, 951.
- Wu, C.-L., Herrington, S.J., Charry, B., Chu, M.L., Knouft, J.H., 2021. Assessing the potential of riparian reforestation to facilitate watershed climate adaptation. *J. Environ. Manag.* 277, 111431.